Copy
RM L55B15

NACA RM L55B15

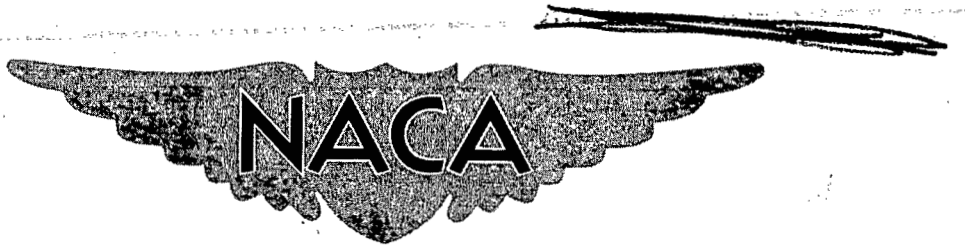

RESEARCH MEMORANDUM

EFFECTS OF A DETACHED TAB ON THE HINGE-MOMENT AND EFFECTIVENESS CHARACTERISTICS OF AN UNSWEPT TRAILING-EDGE CONTROL ON A 60° DELTA WING AT MACH NUMBERS FROM 0.75 TO 1.96

By Odell A. Morris and Gertrude C. Westrick

Langley Aeronautical Laboratory
Langley Field, Va.

NATIONAL ADVISORY COMMITTEE
FOR AERONAUTICS

WASHINGTON

April 14, 1955

NATIONAL ADVISORY COMMITTEE FOR AERONAUTICS

RESEARCH MEMORANDUM

EFFECTS OF A DETACHED TAB ON THE HINGE-MOMENT AND EFFECTIVENESS CHARACTERISTICS OF AN UNSWEPT TRAILING-EDGE CONTROL ON A 60° DELTA WING AT MACH NUMBERS FROM 0.75 TO 1.96

By Odell A. Morris and Gertrude C. Westrick

SUMMARY

An experimental investigation has been conducted in the Langley 9- by 12-inch blowdown tunnel to determine the balancing effects of a detached tab on a constant-chord trailing-edge control mounted on a 60° delta wing at Mach numbers from 0.75 to 1.96. Control hinge moments as well as rolling moments and lift effectiveness of the semispan wing-body combination were obtained for opposed tab and flap deflections up to 15° and for angles of attack of 0° to ±12°.

The results indicated that the ratios of tab to flap deflection required to completely balance out the hinge moments due to 5° flap deflection increased from about -0.4 to nearly -2.0 in the transonic speed range and was essentially constant at -2.0 between Mach numbers of 1.4 and 1.96. For 10° flap deflection, extrapolated data indicated that the required ratios for complete balance would not be much greater than for 5° flap deflection. The loss in rolling-moment effectiveness of the flap-tab combination due to tab deflection required for zero hinge moments at 5° flap deflection varied from about 5 percent to 30 percent as the Mach number was increased from 0.75 to 1.96. The large tab deflections required to balance out the total hinge moments plus the resulting small increments in lift indicate that the detached tab-flap combination would be an ineffective longitudinal control at supersonic speeds.

Comparison of the balancing characteristics of the detached tab with those of a slightly smaller inset tab showed that the tab deflections required to balance the hinge moments due to flap deflection were larger for the inset tab in the transonic range. The rolling-moment effectiveness of the flap with tab deflected for zero hinge moments was generally about 15 percent to 25 percent less for the inset tab than for the detached tab.

INTRODUCTION

The very large hinge moments developed by trailing-edge flap-type controls at transonic and supersonic speeds have encouraged research on various means of balancing such controls aerodynamically. One method of hinge-moment reduction which has been used successfully at low speeds is the balancing or booster tab. However, the limited information available at transonic and low supersonic speeds (for example, refs. 1 and 2) indicates that the balancing effectiveness of trailing-edge flap-tab combinations is considerably reduced in this speed range. It is therefore desirable to obtain additional information on balancing tabs at both transonic and supersonic speeds. In order to furnish such information, an investigation has been carried out in the Langley 9- by 12-inch blowdown tunnel comprising tests on a flap with a $0.040\bar{c}$ inset tab and also on a flap with a $0.050\bar{c}$ detached tab mounted on a 60° delta wing. The results of the tests made on the inset tab are reported in reference 3, and the results of the tests made on the detached tab are presented herein and compared with data of reference 3.

The aerodynamic characteristics of the complete semispan model as well as the hinge-moment characteristics of the flap with the tab were obtained through a flap-deflection range of 0° to 15°, and an angle-of-attack range of 0° to ±12°. The tests were conducted in a transonic nozzle at Mach numbers from 0.75 to 1.31 and average Reynolds numbers from 2.8×10^6 to 3.2×10^6 and in three supersonic nozzles at Mach numbers of 1.41, 1.62, and 1.96 and average Reynolds numbers of 3.0×10^6, 2.8×10^6, and 2.4×10^6, respectively.

SYMBOLS

C_L lift coefficient, Lift/qS

$C_{l_{gross}}$ gross rolling-moment coefficient, (reference axis shown in fig. 1), $\frac{\text{Semispan-model rolling moment}}{2qSb}$

$C_l, \Delta C_L, \Delta C_h$ increment in gross rolling-moment, lift, and hinge-moment coefficient, respectively, due to deflection of flap or tab or both

C_h control hinge-moment coefficient (reference axis is hinge line), $\frac{\text{Hinge moment}}{2qM_{a_1}}$

q	free-stream dynamic pressure, lb/sq in.
S	semispan wing area (including area blanketed by test body), sq in.
S_t	detached-tab area, sq in.
c	local wing chord, in.
$\bar{c}$	mean aerodynamic chord of wing, in.
$\bar{c}_f$	flap chord, in.
b	wing span (twice distance from rolling-moment reference axis to wing tip), in.
b_f	flap span, in.
M_{a_1}	area moment of flap about flap hinge line, $b_f\bar{c}_f^2/2$
M_{a_2}	area moment of flap plus area moment of detached tab about flap hinge line, $M_{a_1} + 1.08S_t$
α	wing angle of attack measured with respect to free stream
δ_f	flap deflection relative to wing chord plane, deg
δ_t	detached-tab deflection relative to flap chord plane, deg
R	Reynolds number based on mean aerodynamic chord of wing
M	Mach number

Subscripts:

α	slope of curve of coefficient plotted against α: $\frac{\partial C_h}{\partial \alpha}$, $\frac{\partial C_L}{\partial \alpha}$, and so forth

δ_f slope of curve of coefficient plotted against δ_f: $\frac{\partial C_h}{\partial \delta_f}$, $\frac{\partial C_l}{\partial \delta_f}$, and so forth

δ_t slope of curve of coefficient plotted against δ_t: $\frac{\partial C_h}{\partial \delta_t}$, $\frac{\partial C_l}{\partial \delta_t}$, and so forth

DESCRIPTION OF MODEL

The principal dimensions of the semispan wing-body combination are given in figure 1(a) and a photograph of the model mounted on the tunnel floor is shown in figure 2. The wing was of delta plan form with 60° leading-edge sweepback and a corresponding aspect ratio of 2.3. A constant-chord trailing-edge flap extended from 0.3 to 0.7 of the wing semispan and was equipped with a constant-chord detached tab mounted on three small booms with a gap equal to $0.414\bar{c}_f$ between the wing trailing edge and the tab leading edge.

The main wing panel was of solid steel and had modified hexagonal airfoil sections with a thickness ratio of 4 percent. The leading edge was modified by a small nose radius as shown in figure 1(a) and the trailing edge tapered from 0.01 inch at the outboard end of the flap to 0.002 inch at the tip. The wing thickness inboard of the control root chord was increased to 0.03c along the 86.7-percent-chord line (see fig. 1) to permit installation of an internal torque rod for use with a strain-gage beam inside the test body.

The flap, which was machined from mild steel, was hinged at 91 percent of the wing root chord, in a line perpendicular to the free air stream. It was attached to the main wing panel by a 0.040-inch-diameter pin at its outboard end, and at its inboard end a 0.095-inch-diameter shaft, integral with the flap, extended through the wing into the test body where it was clamped to an electrical strain-gage beam in the test body. The flap had wedge airfoil sections and its area was 7.5 percent of the half-wing area. The detached tab was also made of mild steel, had double-wedge airfoil sections and its area was 26 percent of the total control area. Small saw-cuts in the tab leading edge alongside each boom permitted the tab deflection to be set by bending the booms at the tab midchord line. The pertinent dimensions of the flap-tab combination are given in figure 1(b).

The fuselage, consisting of a half-body of revolution together with a 0.25-inch shim, was integral with the main wing panel for all tests.

TUNNEL

The tests were conducted in the Langley 9- by 12-inch blowdown tunnel which operates from the compressed air of the Langley 19-foot pressure tunnel. The absolute stagnation pressure of the air entering the test section ranges from 2 to $2\frac{1}{3}$ atmospheres. The compressed air is conditioned to insure condensation-free flow in the test section by being passed through a silica-gel drier and then through banks of finned electrical heaters. Criteria for condensation-free flow were obtained from reference 4. Turbulence-damping screens are located in the settling chamber. A transonic nozzle block provides test-section Mach numbers varying from 0.70 to 1.25, and three supersonic nozzle blocks provide constant test-section Mach numbers of 1.41, 1.62, and 1.96.

Transonic Nozzle

A description of the transonic nozzle, which has a 7- by 10-inch test section, together with a discussion of the flow characteristics obtained from limited calibration tests, is presented in reference 5. Satisfactory test-section flow characteristics are indicated from the minimum Mach number ($M \approx 0.7$) to about $M = 1.20$. The maximum deviations from the average Mach number in the region occupied by the model are shown in figure 3(a). Limited tests indicate that the stream angle probably did not exceed $\pm 0.1^\circ$ at any Mach number. The test-section Mach number decreased as the model angle was changed from 0 to $\pm 12^\circ$. (See fig. 3(b).) The variation with Mach number of the average Reynolds number of the tests is given in figure 3(c) together with the approximate limits of the variation during the test series.

Supersonic Nozzles

Flow conditions in the test section for the three supersonic nozzles were determined from extensive calibration tests and reported in reference 6. Deviations of the flow conditions in the test section with the tunnel clear are presented in the following table:

Average Mach number	1.41	1.62	1.96
Maximum deviation in Mach number	±0.02	±0.01	±0.02
Maximum deviation in stream angle, deg	±0.25	±0.20	±0.20
Average Reynolds number	3.0×10^6	2.8×10^6	2.4×10^6

TEST TECHNIQUE

The semispan model was cantilevered from a five-component strain-gage balance which was set flush with the tunnel floor and was free to rotate through the angle-of-attack range. The aerodynamic forces and moments on the semispan-wing-fuselage combination were measured with respect to the fuselage axis and then rotated to the wind axis. The hinge moments of the flap and tab combination were measured about the flap hinge line by an electrical strain gage in the test body. The 0.25-inch fuselage shim was used to minimize the effects of the tunnel-wall boundary layer on the flow over the fuselage (refs. 7 and 8). A gap of about 0.01 inch was maintained between the test body and the tunnel floor.

CORRECTIONS

No corrections are available to allow for jet-boundary interference and blockage or for reflection-plane effects at high subsonic speeds. Further, reflection of the model shock and expansion waves back to the model by the tunnel walls may appreciably affect the model loadings due to angle of attack at low supersonic Mach numbers but should not appreciably affect the loading due to control deflection. However, comparison of the experimental results obtained in the blowdown tunnel with those obtained in other facilities (ref. 5) indicates the data obtained throughout the Mach number range from 0.7 to 1.2 to be reliable. For detailed discussion see reference 5.

ACCURACY OF DATA

An estimate of the probable errors introduced into the present data by instrument-reading errors, measuring-equipment errors, and calibration errors are presented in the following table:

α, deg	± 0.05
δ_f, deg	± 0.25
δ_t, deg	± 0.4
C_L	± 0.010
C_l	± 0.0010
C_h	± 0.008

The error in δ_f and δ_t given above is the error in the no-load control settings. The change in δ_t due to control loadings is

considered negligible, and for moderate angles of attack the change in δ_f due to control loading is small. However, for high angles of attack the error indicated above for δ_f would be increased, but the increase would probably not exceed 0.8° for any Mach number.

RESULTS

Figure 4 presents the basic aerodynamic coefficients at a Mach number of 0.75 plotted against angle of attack for the 60° delta-wing—fuselage combination for several flap and tab deflections. These data are representative of the basic data and indicate the quality of the data obtained at the other test Mach numbers. Values of rolling-moment coefficient presented in this and subsequent figures have not been corrected for subsonic reflection-plane effects.

Figures 5 and 6 present cross plots of the hinge-moment coefficients against tab deflection for various flap deflections and angles of attack at Mach numbers of 0.75 and 1.41. In some instances, data for the complete tab-deflection and flap-deflection range were not obtained because of the load limitations of the balance and hinge-moment instruments. These data are illustrative of the general character of the curves obtained at the subsonic and supersonic test Mach numbers. Figure 7 presents the variation of hinge-moment coefficients with angle of attack (when $\delta_f = \delta_t = 0^\circ$) for various Mach numbers and the variation of hinge moment and rolling-moment coefficients with flap deflection (when $\alpha = \delta_t = 0^\circ$) for various Mach numbers. The increments in hinge-moment coefficient and the rolling-moment coefficient are plotted against tab deflection in figure 8 for several flap deflections and various Mach numbers at zero angle of attack.

In figure 9 are shown ratios of δ_t/δ_f required for zero hinge moments about the flap hinge line due to flap and tab deflections. The tab could, of course, be used to balance less than 100 percent of the control hinge moments due to deflection; however, ratios of δ_t/δ_f for $\Delta C_h = 0$ provide a convenient parameter for comparison of the tab balancing effectiveness at various Mach numbers. These ratios are compared in figure 10 with those for an inset tab tested on the same wing and reported in reference 3. The ratios of δ_t/δ_f required to balance the total hinge moments due to angle of attack, flap deflection, and detached-tab deflection are shown in figure 11. These ratios were obtained from the curves of figures 5 and 6 and similar cross plots. In all figures the ratios given at negative angles of attack and positive deflections are equivalent to those for positive angles of attack and negative deflections by reason of model symmetry.

The rolling-moment coefficients corresponding to the angle conditions of figure 9 are shown in figure 12, and increments in lift coefficient due to control deflections corresponding to the angle conditions of figure 11 are shown in figure 13. Ratios of the rolling moment of the flap with tab deflected for $\Delta C_h = 0$ to that of the flap with tab undeflected are shown in figure 14 and compared with those of the inset tab of reference 3 for various angles of attack and flap deflections. Figure 15 shows a comparison of the variation with Mach number of the hinge-moment slope parameters for the detached tab and the inset tab. Also, figure 16 shows a comparison of the variation with Mach number of some flap and tab rolling-moment effectiveness parameters for the two tabs.

DISCUSSION

Control Hinge Moments

Figure 9 shows that the tab was capable of reducing to zero the hinge moments due to 5° flap deflection throughout the complete Mach number range. The required ratio for 5° flap deflection increased from about -0.4 to -2.0 for Mach numbers from 0.85 to 1.4. Above $M = 1.4$ the ratios were essentially constant with Mach number, being slightly less than -2.0 for positive angles of attack and flap deflection and a little greater than -2.0 for angles of attack and flap deflection of opposite sign. The increases in δ_t/δ_f at transonic speeds were due to the fact that the increase in the slope parameter $C_{h_{\delta_f}}$ was accompanied by a decrease in the slope parameter $C_{h_{\delta_t}}$ (see figs. 7, 8, and 15). The increase in $C_{h_{\delta_f}}$ was associated with the rearward shift in center of pressure of the control in the transonic range. However, $C_{h_{\delta_t}}$ did not increase similarly, apparently because any change in the length of the moment arm of the tab loading due to the center-of-pressure shift was insufficient to overcome the decrease in tab loading in this speed range.

Figure 9 also shows that increasing the flap deflection from 5° to 10° slightly increased the values of δ_t/δ_f required for zero flap hinge moments at subsonic speeds as a result of the increase in slope $C_{h_{\delta_f}}$ with increases in flap deflection (see figs. 5 and 7(a)). At Mach numbers greater than 1.0 the data for 10° flap deflection are limited by the range of tab deflections tested. It appears, however, that the required ratios for 10° flap deflection would not be much greater than for 5° flap deflection, since figure 8 shows the slope of the hinge-moment variation with tab deflection to be nearly constant with tab

deflection and only slightly less at 10° flap deflection than at 5°. This may not be true for angles of attack of opposite sign ($\delta_f = 10°$; $\alpha = -4°$ and $-8°$) since figure 6 shows some decrease in slope $\left(C_{h_{\delta_t}}\right)$ for $M = 1.41$ at the larger tab and flap deflections.

A comparison is shown in figure 10 of the values of δ_t/δ_f required to produce zero hinge moments for the detached tab and for the inset tab of reference 3. The area of the inset tab was 29 percent of the total control area (tab area included), whereas the detached-tab area was 26 percent of the total control area or 36 percent of the flap-alone area. The values of δ_t/δ_f for the detached tab and the inset tab (fig. 10) generally showed little differences in the tab deflection required to balance the hinge moments for 5° flap deflection except in the transonic speed range. Here the increase in δ_t/δ_f for the detached tab was delayed to a higher Mach number at angles of attack less than 8°. The reason for the smaller values of δ_t/δ_f for the detached tab in the transonic range can be demonstrated by basing the hinge-moment slope coefficients on the total moment area of the flap plus tab as shown in figure 15. The values of $C_{h_{\delta_t}}$ for the detached tab are then very nearly equal to those for the inset tab through the entire Mach number range, whereas the values of $C_{h_{\delta_f}}$ are appreciably smaller for the detached tab at Mach numbers in the transonic range.

Calculations based on the two-dimensional small-perturbation theory of reference 9 and neglecting second-order terms (control loadings are assumed to be proportional to control deflection) predict values of δ_t/δ_f at supersonic speeds of -2.0 and -1.9 for the inset and detached tab, respectively. These predictions are within 5 percent of the experimental values of δ_t/δ_f for both tabs between Mach numbers of 1.3 and 2.0 when $\alpha = 0$ and $\delta_f = 5°$, although the 5-percent difference in the calculated values for the two tabs is not shown by experiment. It is interesting to note that calculations made for the inset tab in reference 3 by use of three-dimensional linearized theory differed from experiment by 15 percent.

For the detached tab, the values of δ_t/δ_f required to balance 10° flap deflection were generally less than for the inset tab throughout the Mach number range, although the differences were small at the lowest Mach numbers and at $\alpha = 8°$. The values of δ_t/δ_f shown for the detached tab at supersonic Mach numbers (short-dash line in fig. 10) were obtained by extrapolation and should be viewed with caution when values exceed -2.0. The larger ratios shown for the inset tab were generally due to decreased

balancing effectiveness of the tab with increased tab deflection. In fact, reference 3 showed that the hinge moments for flap deflections much above 10° could not be 100-percent balanced by the inset tab because of this decreased effectiveness. It appears that the detached tab would be capable of 100-percent balance of hinge moments for flap deflections somewhat higher than possible for the inset tab; however, the limited tab-deflection range of the present tests does not permit definition of this limit. Also, as was pointed out in reference 3, reducing the balance required would increase proportionally the usable flap-deflection range. It is interesting to note that at supersonic speeds the values of δ_t/δ_f are smallest at the higher angles of attack for both tabs at 5° and 10° flap deflection and increase with decreasing angle of attack.

The data of figure 11 show that, for Mach numbers less than 1.0, the detached tab was easily capable of balancing the total control hinge moments due to angle of attack and deflection for both 5° and 10° flap deflections and for all angles of attack tested. Above $M = 1.00$, however, the value of δ_t/δ_f required for 5° flap deflection increased rapidly with angle of attack and quickly became too large to balance the total control hinge moments. At Mach numbers less than 1.0, little change in δ_t/δ_f with angle of attack was shown until $\alpha = 12°$ was reached. This behavior resulted from the nonlinear variation of hinge moment with angle of attack (see figs. 4(c) and 7(b)) with no large increase in hinge moment below $\alpha = 10°$. These nonlinearities were apparently a result of the addition of the tab or supporting beams, since the variation of hinge moment with angle of attack for the flap without tab (ref. 3) was essentially linear at Mach numbers less than 1.0.

For angles of attack and flap deflection of opposite sign, the angle-of-attack and flap-deflection loadings oppose each other and the values of δ_t/δ_f were somewhat smaller. At larger negative angles of attack, however, the ratios would become very large positively.

Control Effectiveness

Figure 12 shows that the values of rolling-moment coefficient for the flap and tab deflected to give $\Delta C_h = 0$ were a maximum at subsonic Mach numbers, decreased rapidly with increasing Mach number in the transonic range, and then decreased less rapidly at supersonic Mach numbers. The rate of decrease of C_l with Mach number corresponded roughly to the rate of increase of δ_t/δ_f with Mach number in figure 9. However, the decrease in C_l for $\Delta C_h = 0$ was not entirely due to tab deflection, for the rolling effectiveness of plain flap-type controls also decreases rapidly in the transonic speed range. Figure 14, which includes data

from reference 3 on the inset tab, is presented to show the loss in rolling effectiveness due to tab deflection. In general, the rolling-moment coefficient for $\Delta C_h = 0$ was about 95 percent of the rolling-moment coefficient for $\delta_t = 0$ at subsonic Mach numbers and decreased to about 70 percent at supersonic Mach numbers for 5° flap deflection and positive angles of attack. This compared with 80 percent and 50 percent rolling effectiveness for the inset-tab—flap combination at subsonic and supersonic Mach numbers, respectively. For negative angles of attack and 10° flap deflection the ratios were generally about 5 percent to 15 percent lower for both tabs, with the largest decreases usually shown in the supersonic Mach number range.

The greater rolling-moment effectiveness shown for the detached-tab—flap combination appears to result from the fact that the tab rolling effectiveness is generally less for the detached tab than for the inset tab. Figure 16, which presents the variation with Mach number of some flap and tab rolling-moment effectiveness parameters, shows that tab rolling effectiveness, $C_{l_{\delta_t}}$, for the detached-tab—flap combination is nearly constant throughout the speed range and very much less at subsonic Mach numbers than that of the inset tab. The higher rolling effectiveness for the inset tab at subsonic speeds probably was caused by an induced loading on the wing due to tab deflection, whereas the detached tab causes no induced loading on the wing. However, the difference in $C_{l_{\delta_f}}$ for the two controls with tab undeflected, which must be due to the presence of the detached tab and supporting booms, is of about the same order as $C_{l_{\delta_t}}$ for the detached tab at all test Mach numbers. A comparison of the slope effectiveness parameter $C_{l_{\delta_f}}$ (for $\Delta C_h = 0$) for the two tabs shows a larger difference in the magnitudes of the two slopes at subsonic speeds; however, a larger percentage change occurs in the supersonic range as shown by the ratio of $C_{l_{\delta_f}}$ (for $\Delta C_h = 0$) to $C_{l_{\delta_f}}$ (for $\delta_t = 0$).

The data of figure 13 show that at subsonic speeds adequate lift effectiveness was obtained at all angles of attack and for both 5° and 10° flap deflections. However, at supersonic speeds, the large tab deflections required to balance out the total control hinge moment (see fig. 11) plus the small increments in lift resulting from flap and tab deflections indicate that the detached-tab—flap combination would be an ineffective longitudinal control at supersonic speeds.

CONCLUSIONS

An investigation to determine the balance characteristics of a detached tab on a trailing-edge flap-type control mounted on a 60° delta wing was conducted in the Langley 9- by 12-inch blowdown tunnel through a Mach number range of 0.75 to 1.96. The following results were indicated:

1. The ratio of the tab to flap deflection required to completely balance out the hinge moments due to 5° flap deflection increased from about -0.5 to nearly -2.0 in the transonic speed range and was essentially constant at -2.0 between Mach numbers of 1.4 and 1.96. For 10° flap deflection, extrapolated data indicated that the required ratios for complete balance would not be much greater than for 5° flap deflection.

2. The loss in rolling-moment effectiveness of the flap-tab combination due to tab deflection required for zero hinge moment at 5° flap deflection varied from about 5 percent to 30 percent as the Mach number was increased from 0.75 to 1.96.

3. The large tab deflections required to balance out the total hinge moments plus the resulting small increments in lift indicate that the detached-tab—flap combination would be an ineffective longitudinal control at supersonic speeds.

4. Comparison of the balancing characteristics of the detached tab with those of a slightly smaller inset tab showed that the tab deflections required to balance the hinge moments due to flap deflection were larger for the inset tab in the transonic range. The rolling-moment effectiveness of the flap with tab deflected for zero hinge moments was generally about 15 percent to 25 percent less for the inset tab than for the detached tab.

Langley Aeronautical Laboratory,
National Advisory Committee for Aeronautics,
Langley Field, Va., January 28, 1954.

REFERENCES

1. Lockwood, Vernard E., and Fikes, Joseph E.: Preliminary Investigation at Transonic Speeds of the Effect of Balancing Tabs on the Hinge-Moment and Other Aerodynamic Characteristics of a Full-Span Flap on a Tapered 45° Sweptback Wing of Aspect Ratio 3. NACA RM L52A23, 1952.

2. Bland, William M., Jr., and Marley, Edward T.: A Free-Flight Investigation at Zero Lift in the Mach Number Range Between 0.7 and 1.4 To Determine the Effectiveness of an Inset Tab as a Means of Aerodynamically Relieving Aileron Hinge Moments. NACA RM L52K07, 1952.

3. Guy, Lawrence D., and Brown, Hoyt V.: Effects of an Inset Tab on the Hinge-Moment and Effectiveness Characteristics of an Unswept Trailing-Edge Control on a 60° Delta Wing at Mach Numbers From 0.75 to 1.96. NACA RM L54K16a, 1955.

4. Burgess, Warren C., Jr., and Seashore, Ferris L.: Criterions for Condensation-Free Flow in Supersonic Tunnels. NACA TN 2518, 1951.

5. Guy, Lawrence D.: Effects of Overhang Balance on the Hinge-Moment and Effectiveness Characteristics of an Unswept Trailing-edge Control on a 60° Delta Wing at Transonic and Supersonic Speeds. NACA RM L54G12a, 1954.

6. May, Ellery B., Jr.: Investigation of the Effects of Leading-Edge Chord-Extensions on the Aerodynamic and Control Characteristics of Two Sweptback Wings at Mach Numbers of 1.41, 1.62, and 1.96. NACA RM L50L06a, 1951.

7. Conner, D. William: Aerodynamic Characteristics of Two All-Movable Wings Tested in the Presence of a Fuselage at a Mach Number of 1.9. NACA RM L8H04, 1948.

8. Mitchell, Meade H., Jr.: Effects of Varying the Size and Location of Trailing-Edge Flap-Type Controls on the Aerodynamic Characteristics of an Unswept Wing at a Mach Number of 1.9. NACA RM L50F08, 1950.

9. The Staff of the Ames 1- by 3-Foot Supersonic Wind-Tunnel Section: Notes and Tables for Use in the Analysis of Supersonic Flow. NACA TN 1428, 1947.

[redacted]

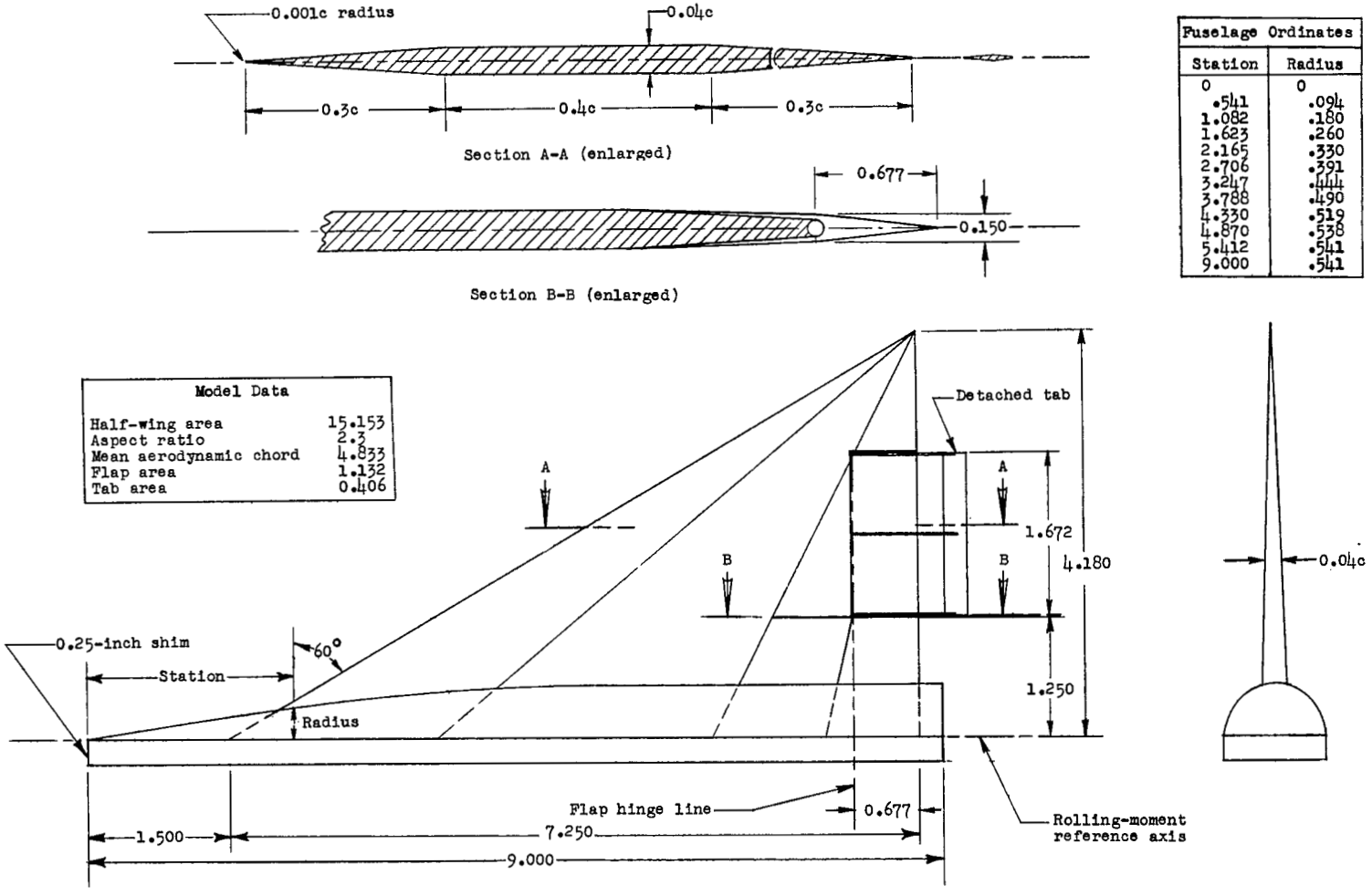

Fuselage Ordinates	
Station	Radius
0	0
.541	.094
1.082	.180
1.623	.260
2.165	.330
2.706	.391
3.247	.444
3.788	.490
4.330	.519
4.870	.538
5.412	.541
9.000	.541

(a) Wing-fuselage combination.

Figure 1.- Details of semispan wing-fuselage model (all dimensions are in inches).

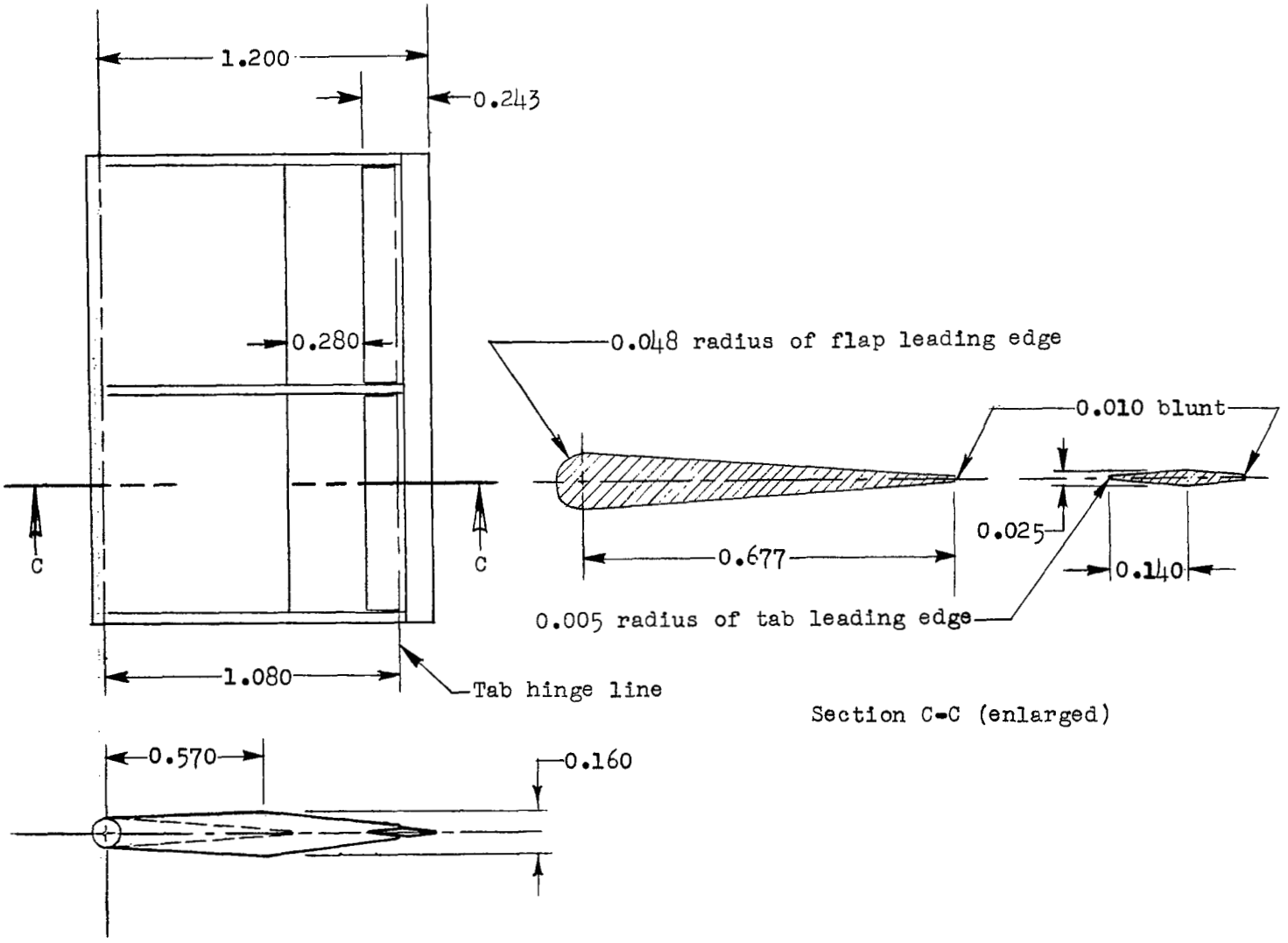

(b) Flap and detached tab.

Figure 1.- Concluded.

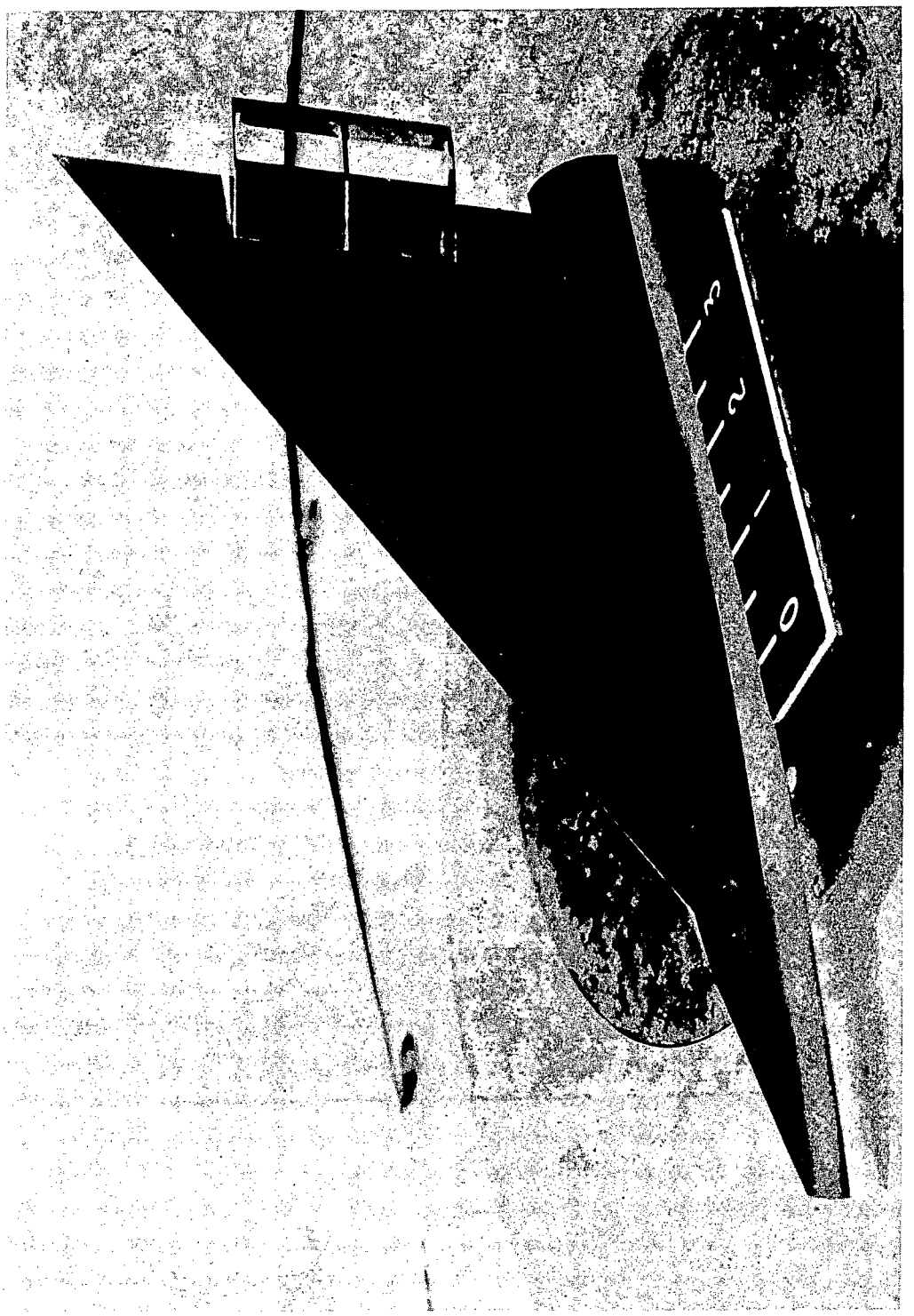

L-80535.1

Figure 2.- Photograph of 60° delta-wing—fuselage combination.

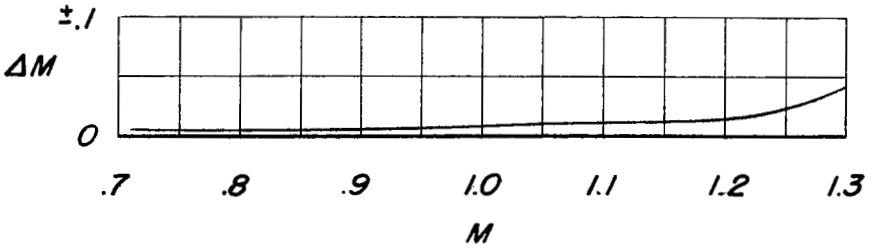

(a) Maximum deviation from average test-section Mach number.

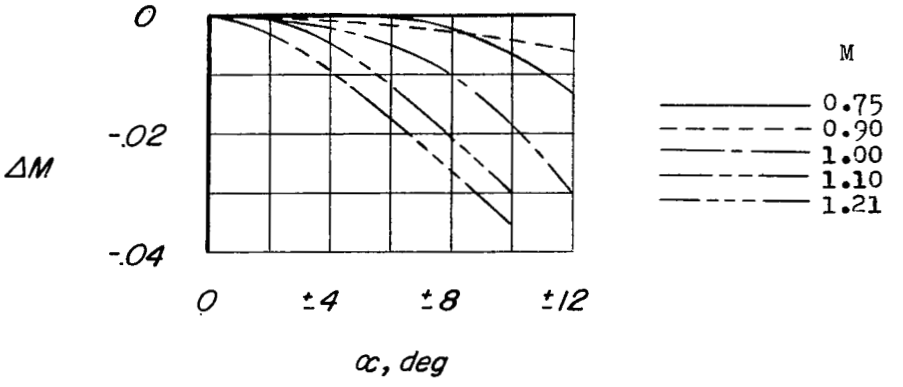

(b) Maximum variation of test-section Mach number with angle of attack.

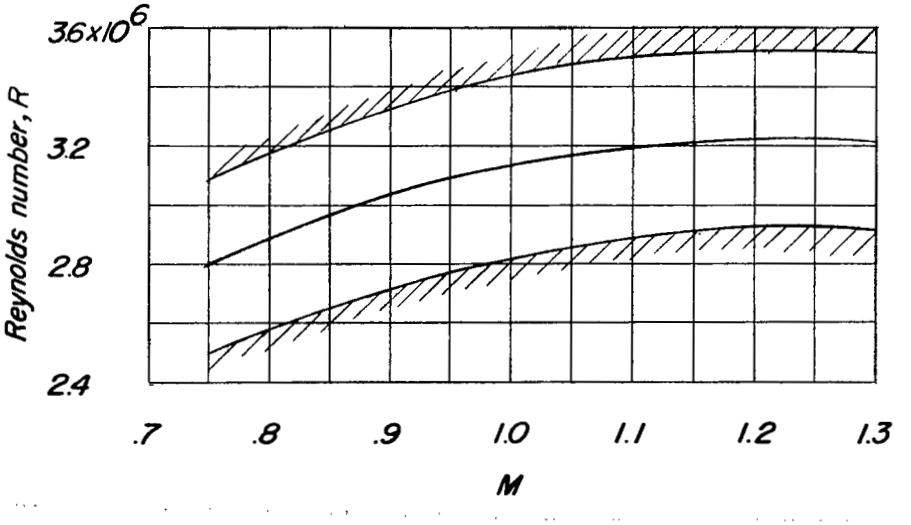

(c) Variation of test Reynolds number with Mach number for 60° delta wing.

Figure 3.- Flow characteristics of transonic nozzle.

[redacted]

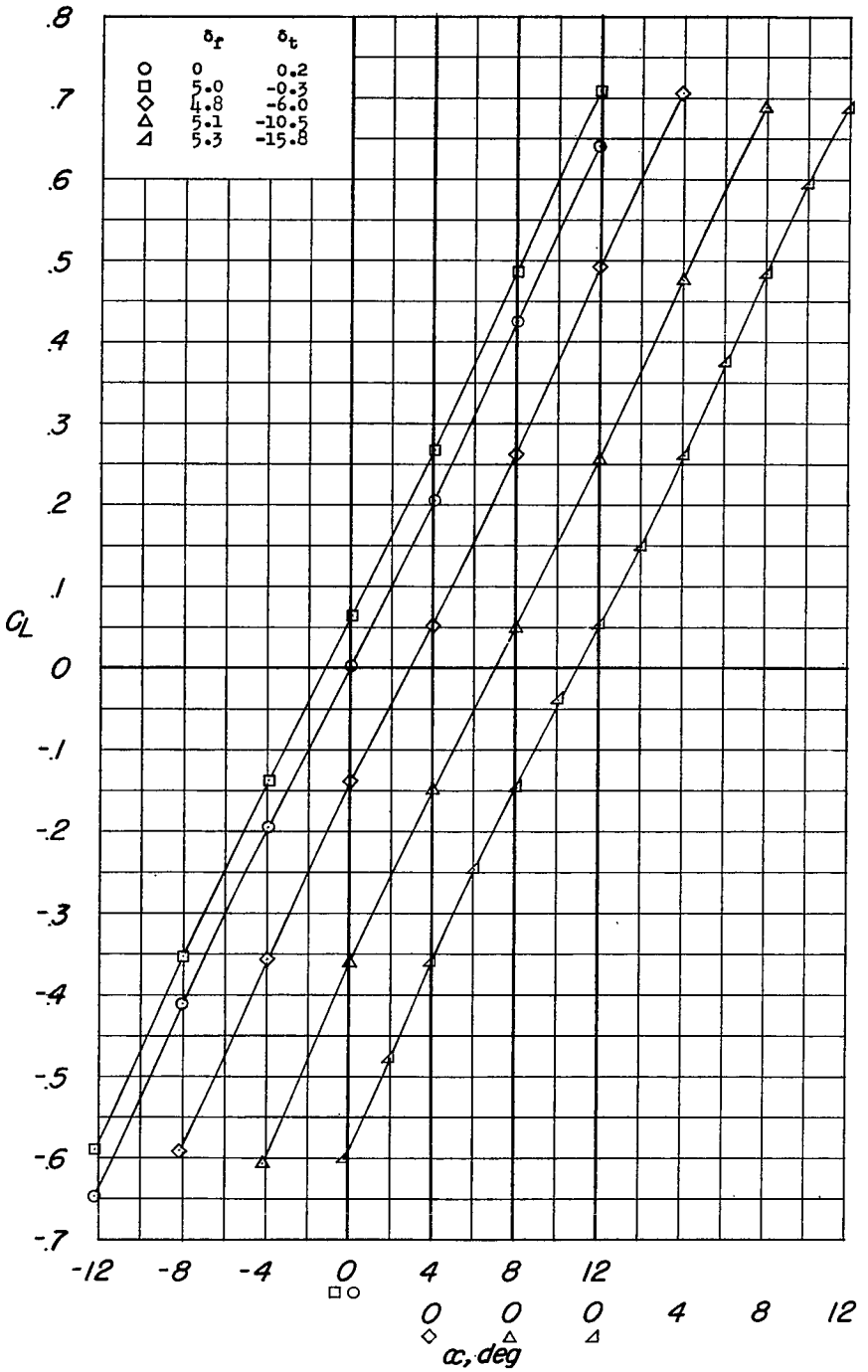

(a) C_L against α.

Figure 4.- Aerodynamic characteristics of a 60° delta-wing—body combination and trailing-edge flap equipped with a detached tab for various flap and tab deflections at a Mach number of 0.75.

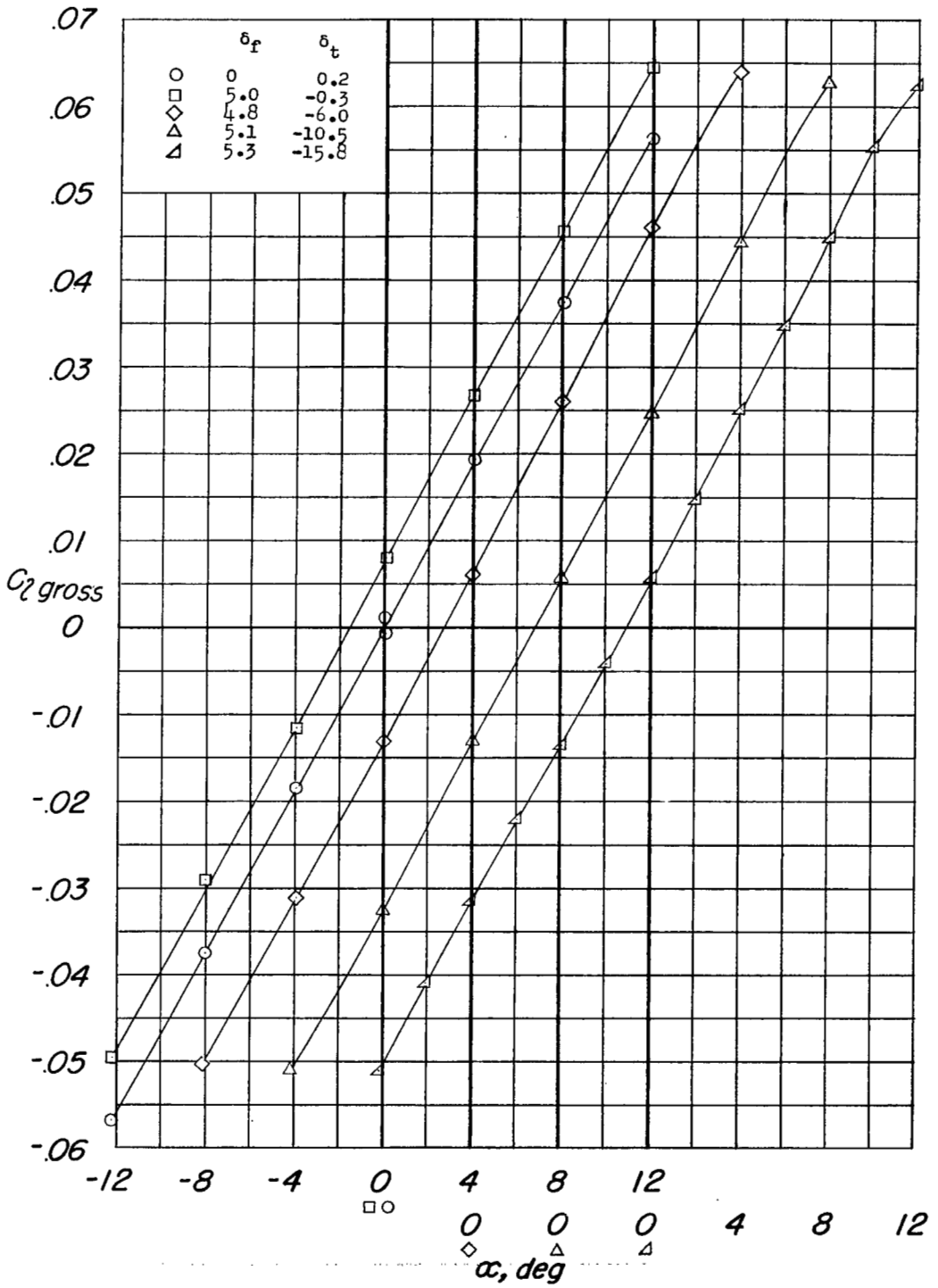

(b) $C_{l_{gross}}$ against α.

Figure 4.- Continued.

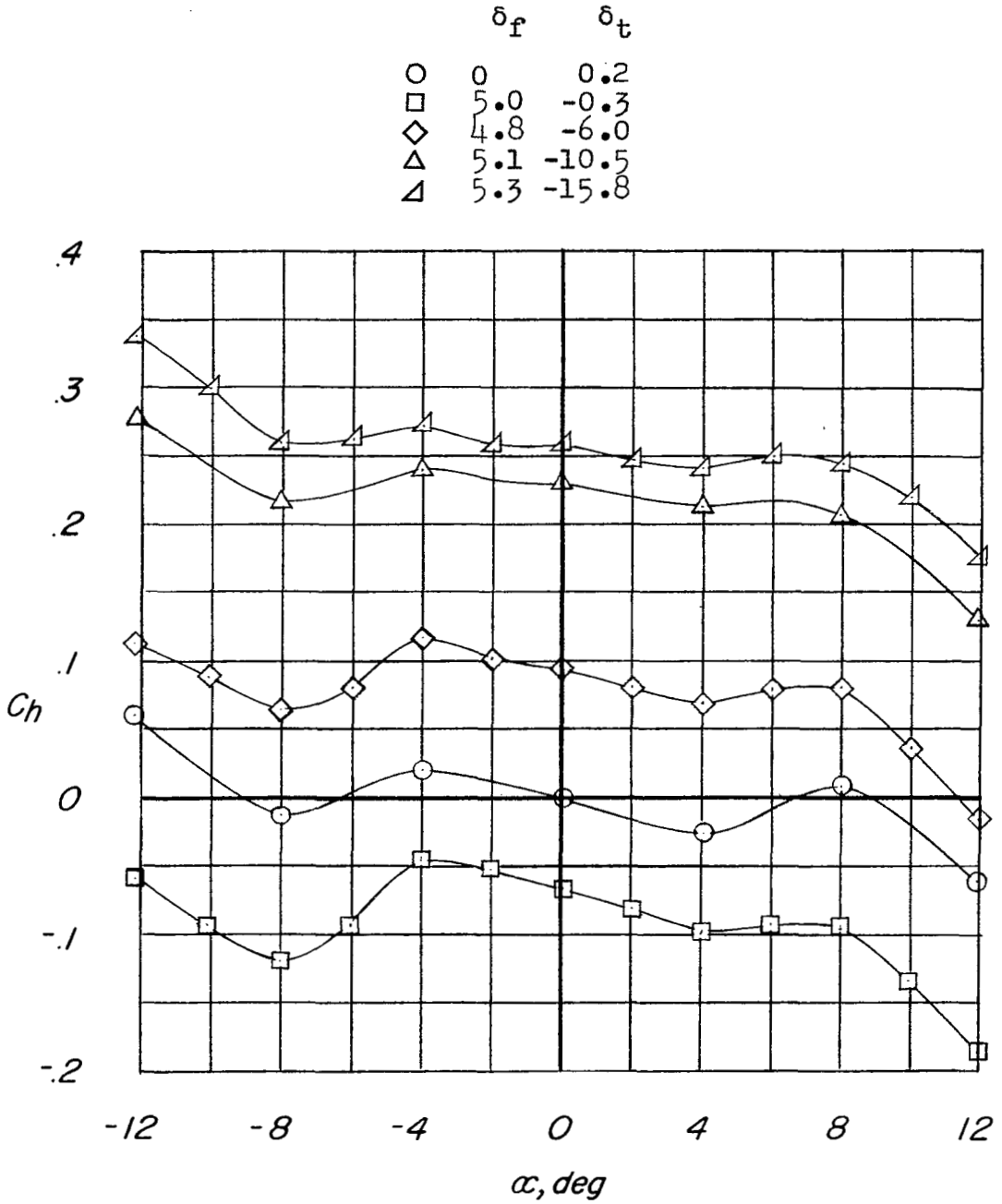

(c) C_h against α.

Figure 4.- Concluded.

[redacted]

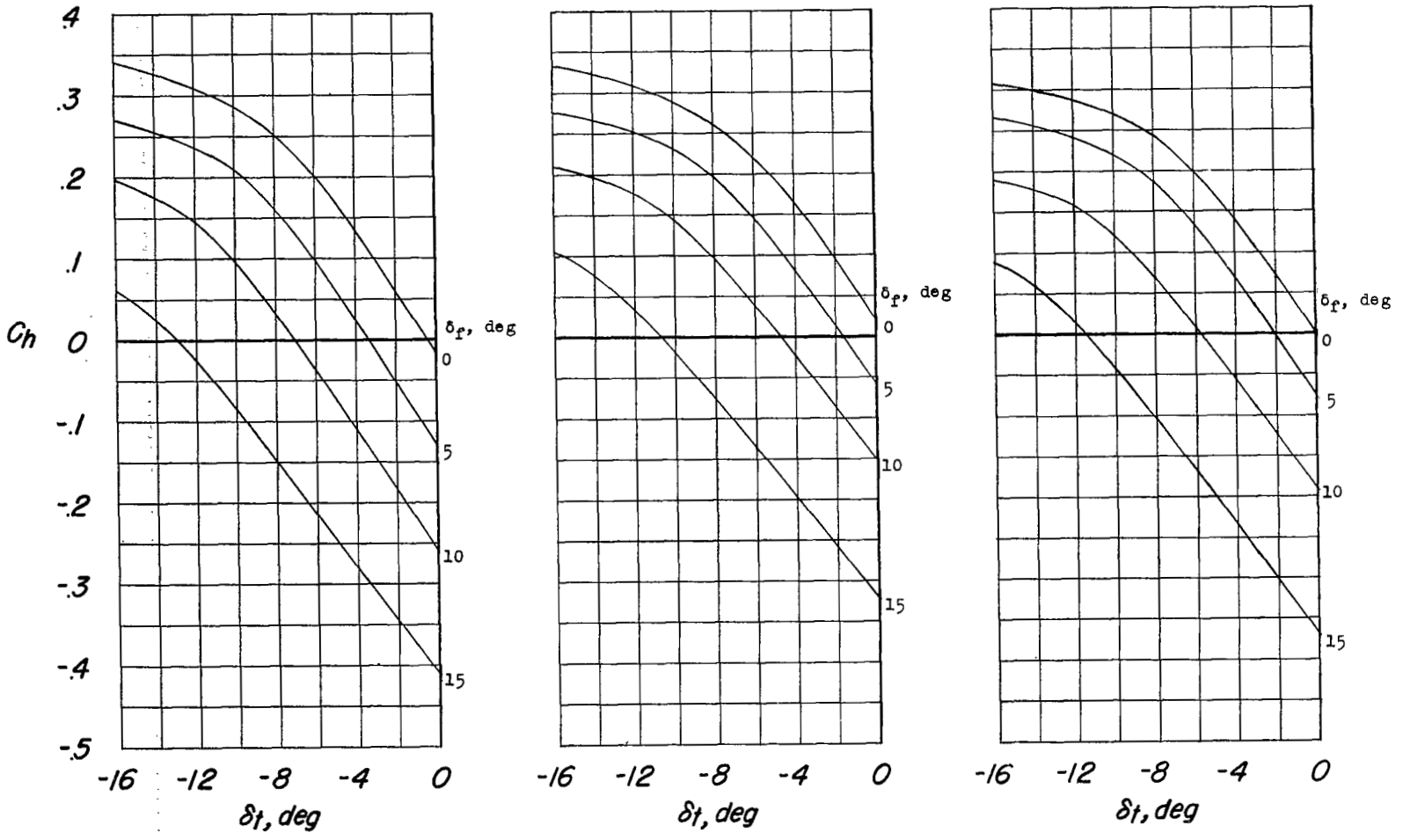

(a) $\alpha = -8^\circ$. (b) $\alpha = -4^\circ$. (c) $\alpha = 0^\circ$.

Figure 5.- Variation of hinge-moment coefficient with tab deflection for various flap deflections and angles of attack at a Mach number of 0.75.

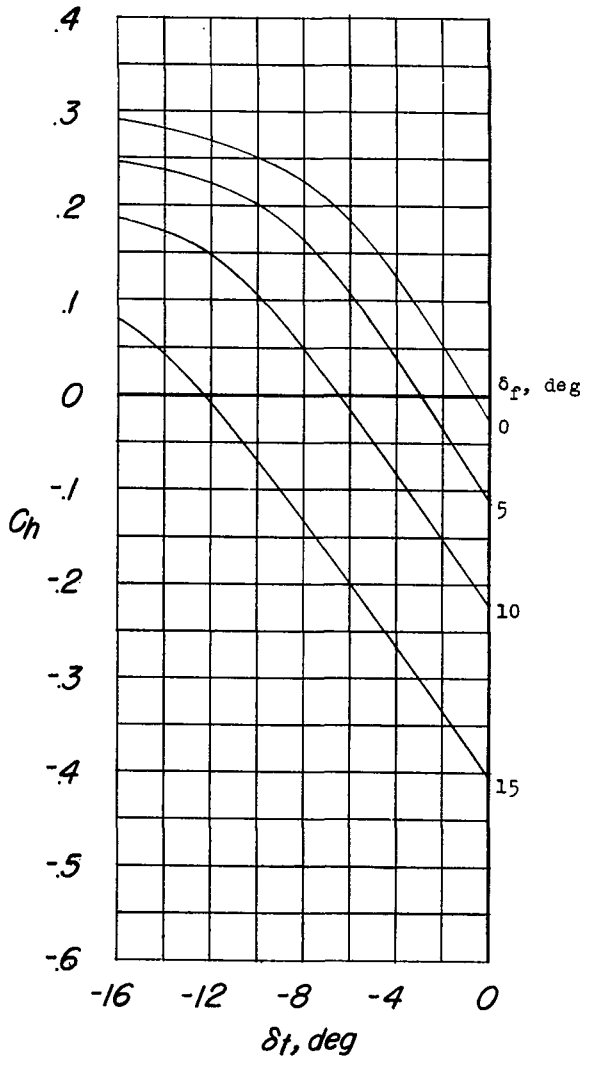

(d) $\alpha = 4^\circ$.

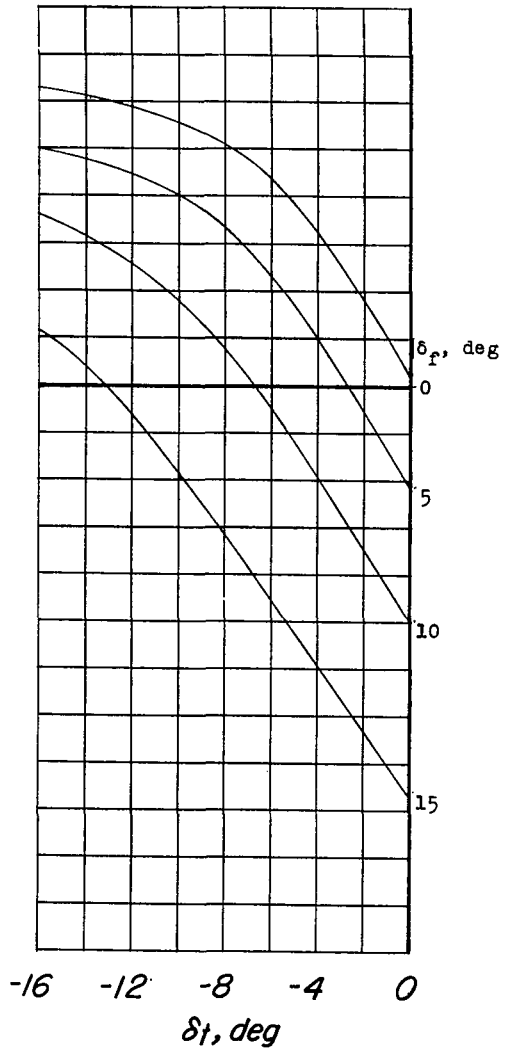

(e) $\alpha = 8^\circ$.

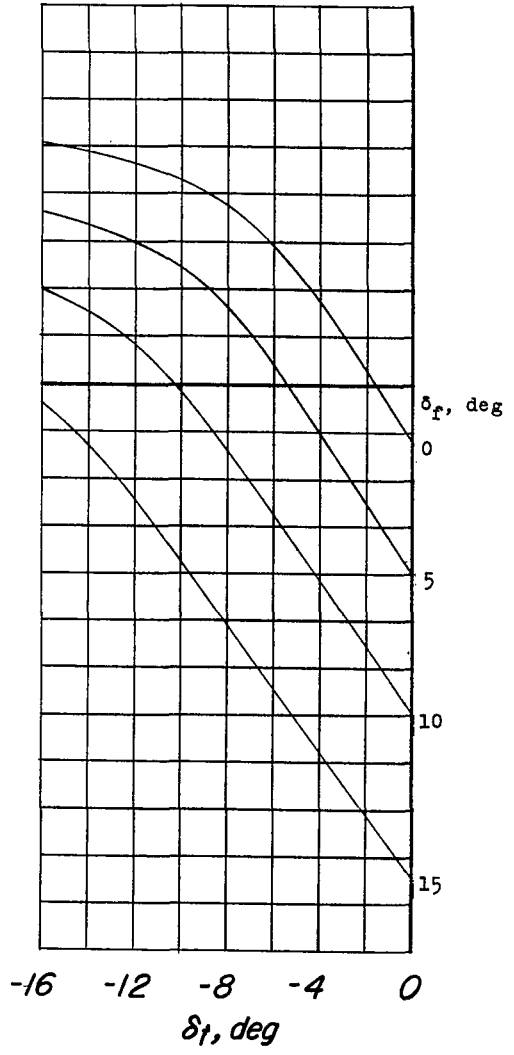

(f) $\alpha = 12^\circ$.

Figure 5.- Concluded.

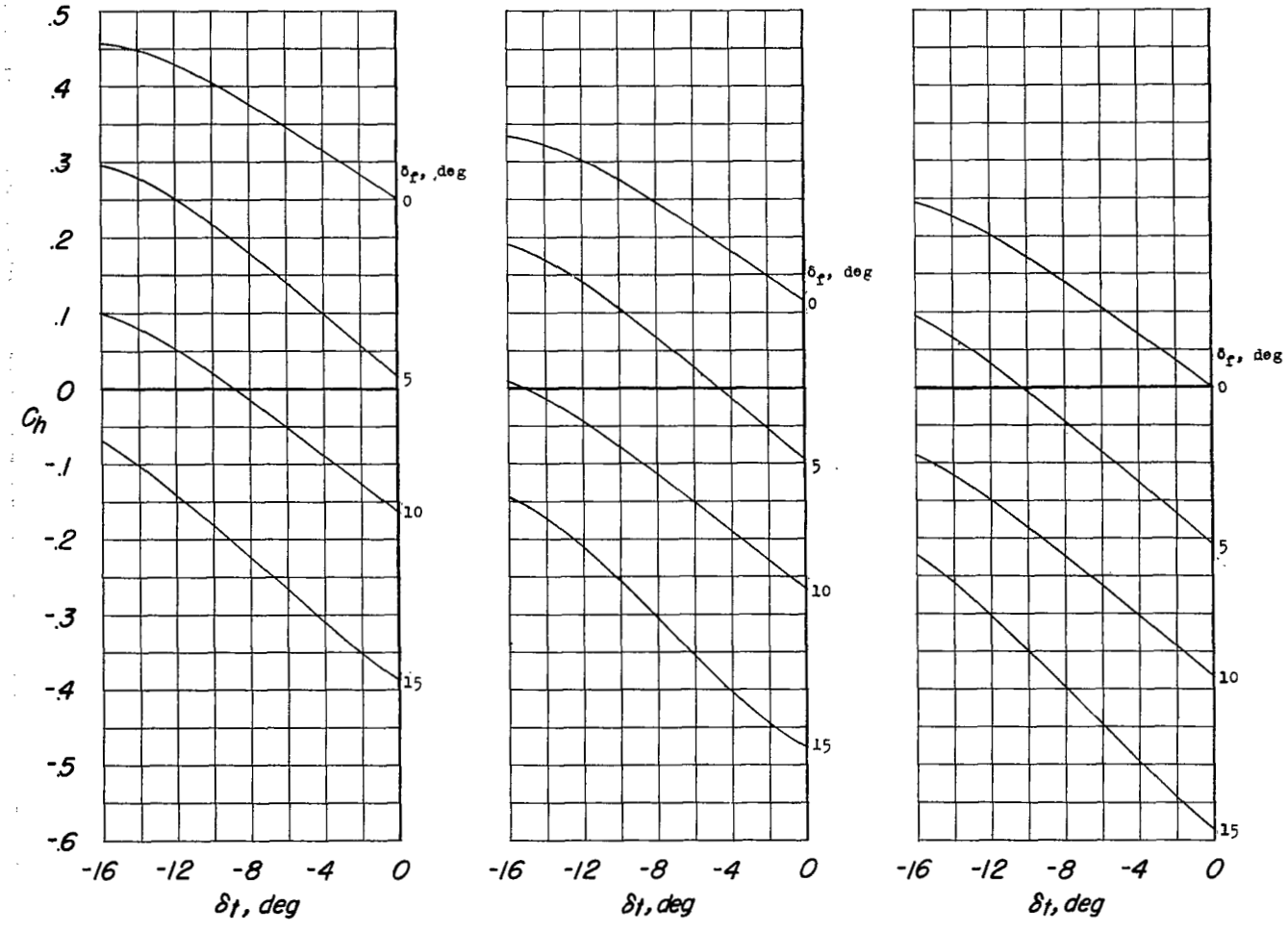

(a) $\alpha = -8^\circ$. (b) $\alpha = -4^\circ$. (c) $\alpha = 0^\circ$.

Figure 6.- Variation of hinge-moment coefficient with tab deflection for various flap deflections and angles of attack at a Mach number of 1.41.

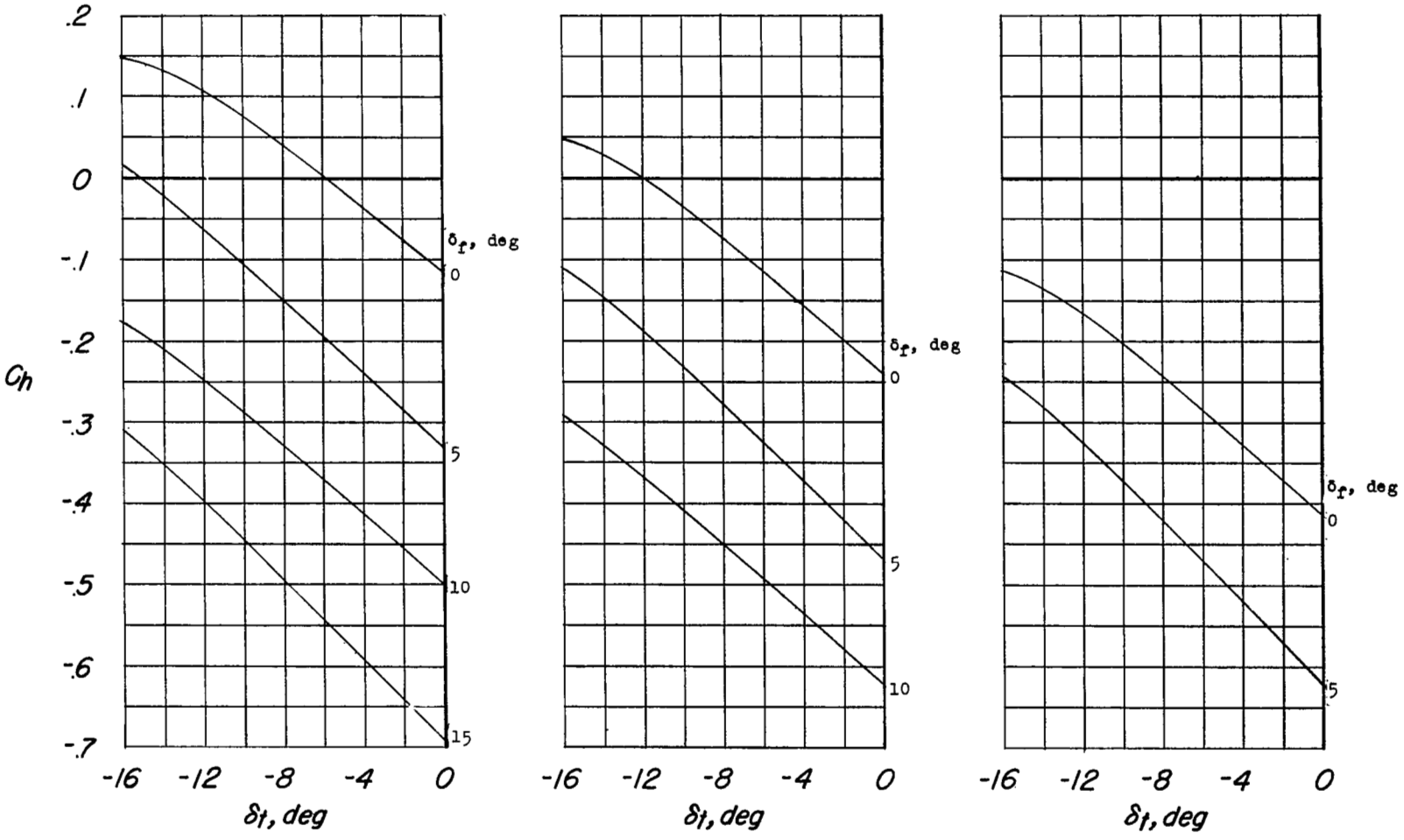

(d) $\alpha = 4^\circ$.

(e) $\alpha = 8^\circ$.

(f) $\alpha = 12^\circ$.

Figure 6.- Concluded.

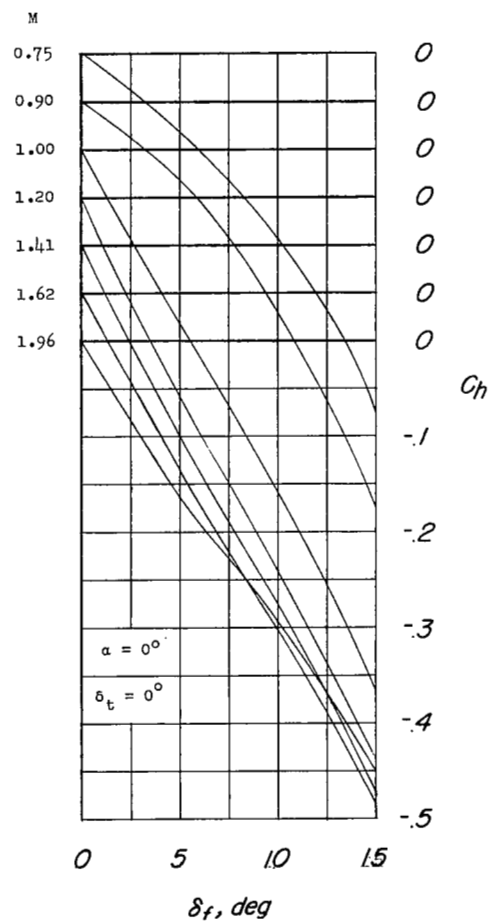

(a) C_h against δ_f.

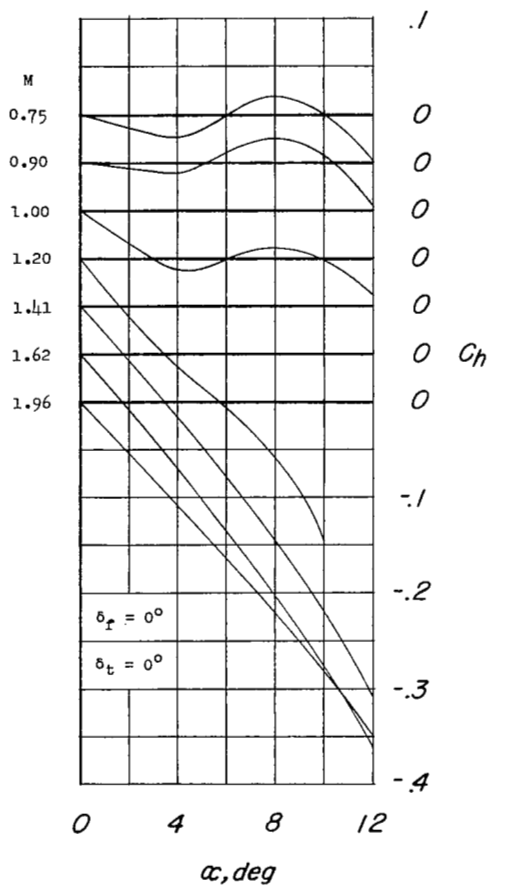

(b) C_h against α.

Figure 7.- Variation of hinge-moment coefficient and rolling-moment coefficient with flap deflection and angle of attack for various Mach numbers.

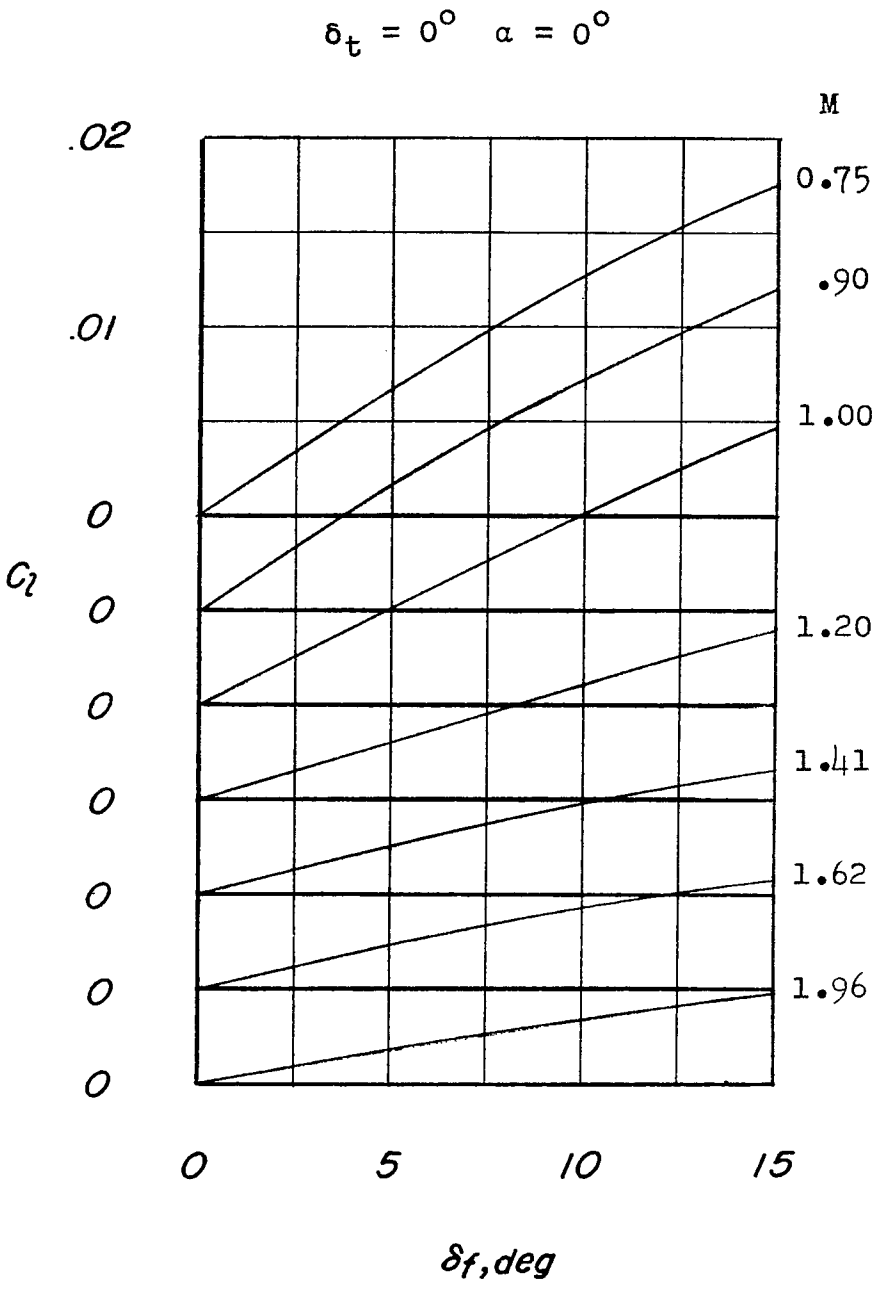

(c) C_l against δ_f.

Figure 7.- Concluded.

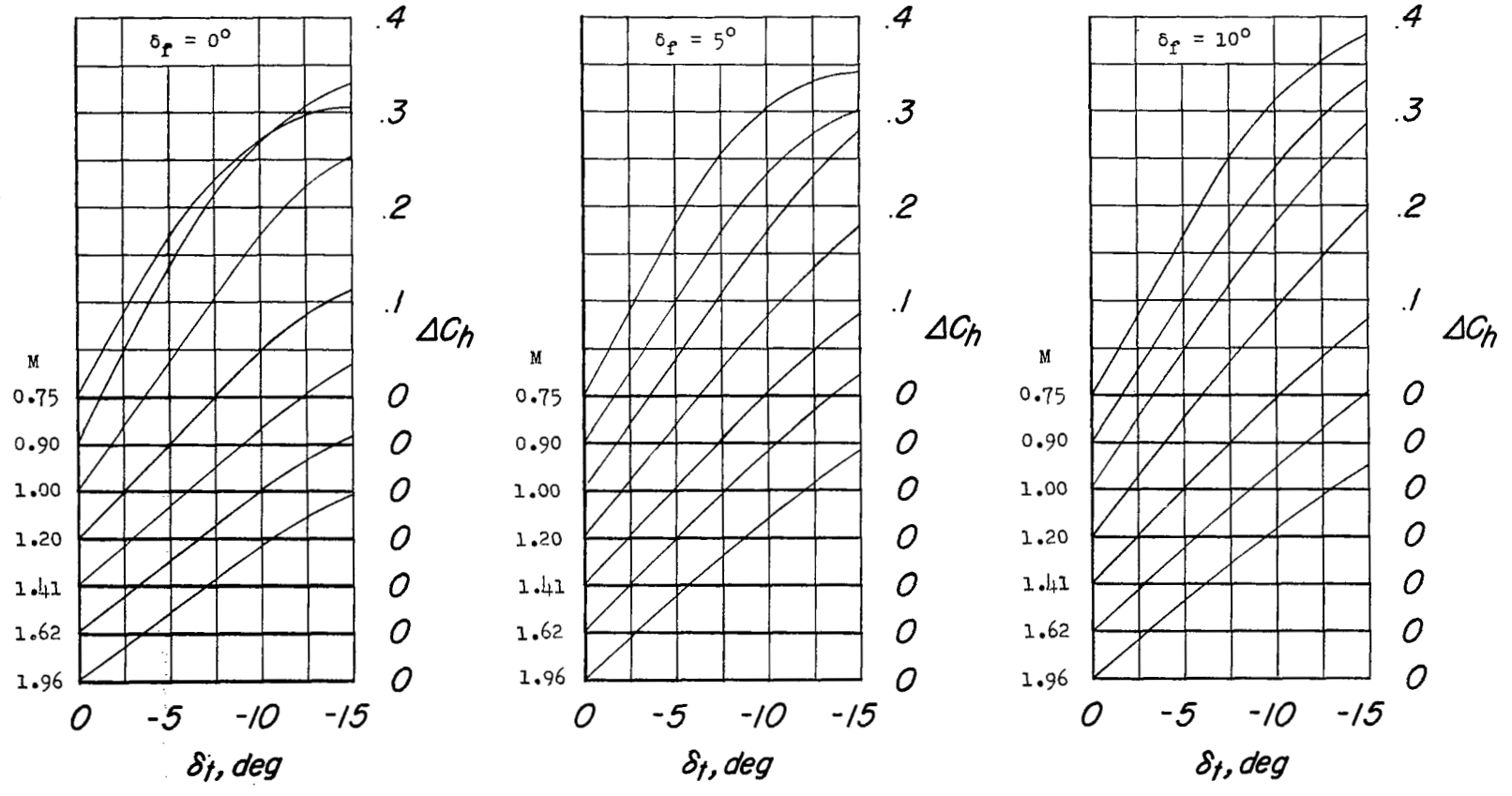

(a) ΔC_h against δ_t.

Figure 8.- Increment in hinge-moment coefficient and rolling-moment coefficient due to tab deflection plotted against tab deflection for various flap deflections and Mach numbers. $\alpha = 0°$.

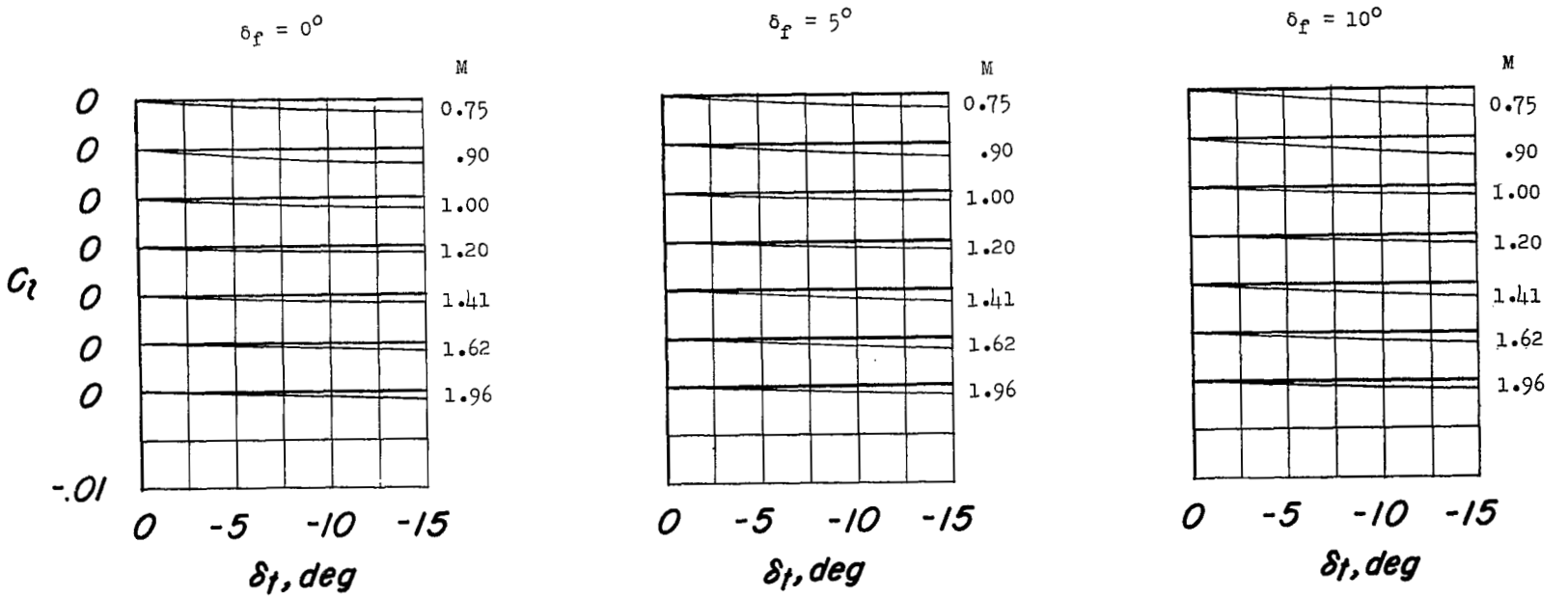

(b) C_l against δ_t.

Figure 8.- Concluded.

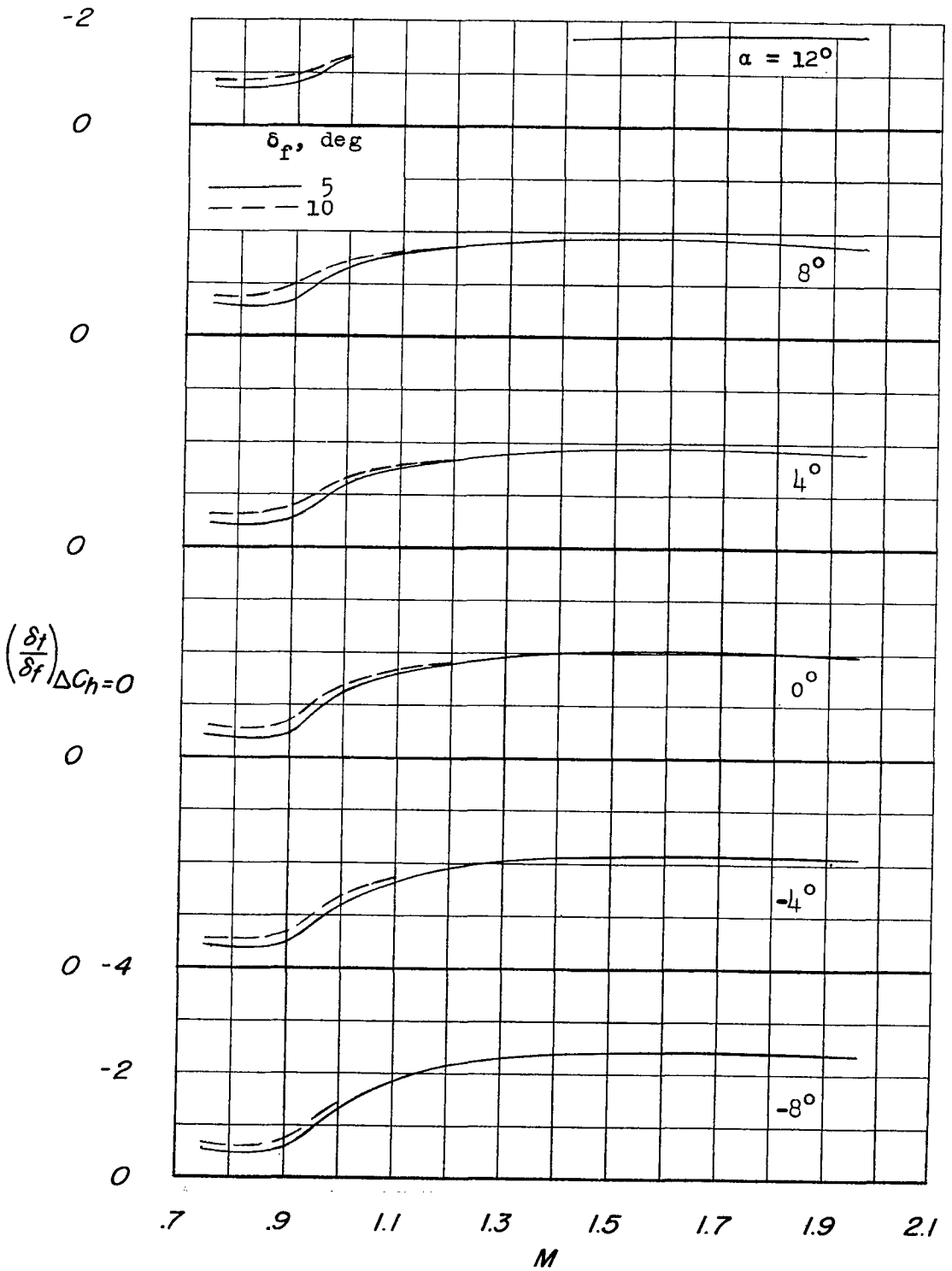

Figure 9.- Variation with Mach number of the ratio of tab deflection to flap deflection required for $\Delta C_h = 0$.

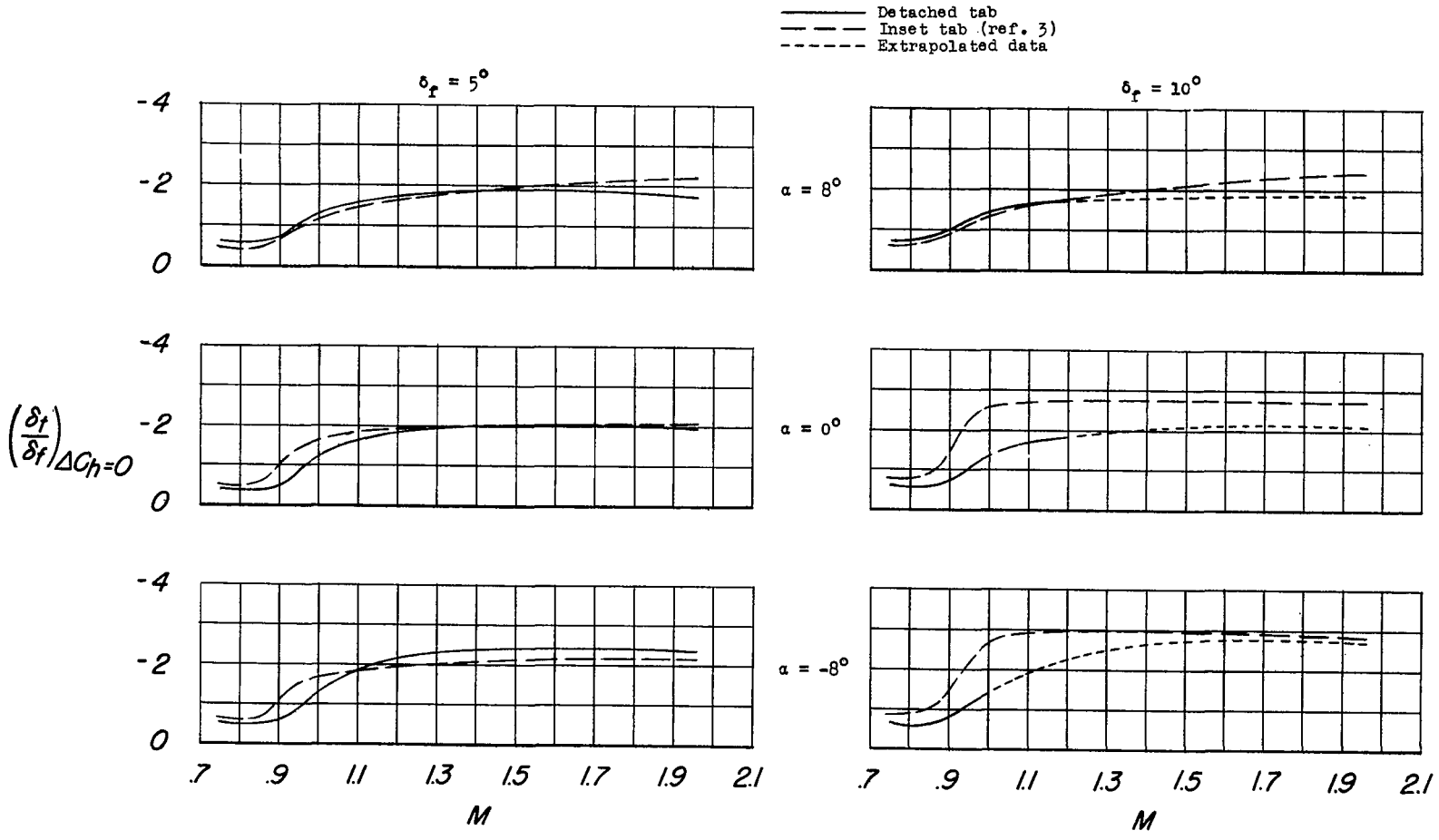

Figure 10.- Variation of δ_t/δ_f with Mach number for the detached tap and for an inset tab when $\Delta C_h = 0$.

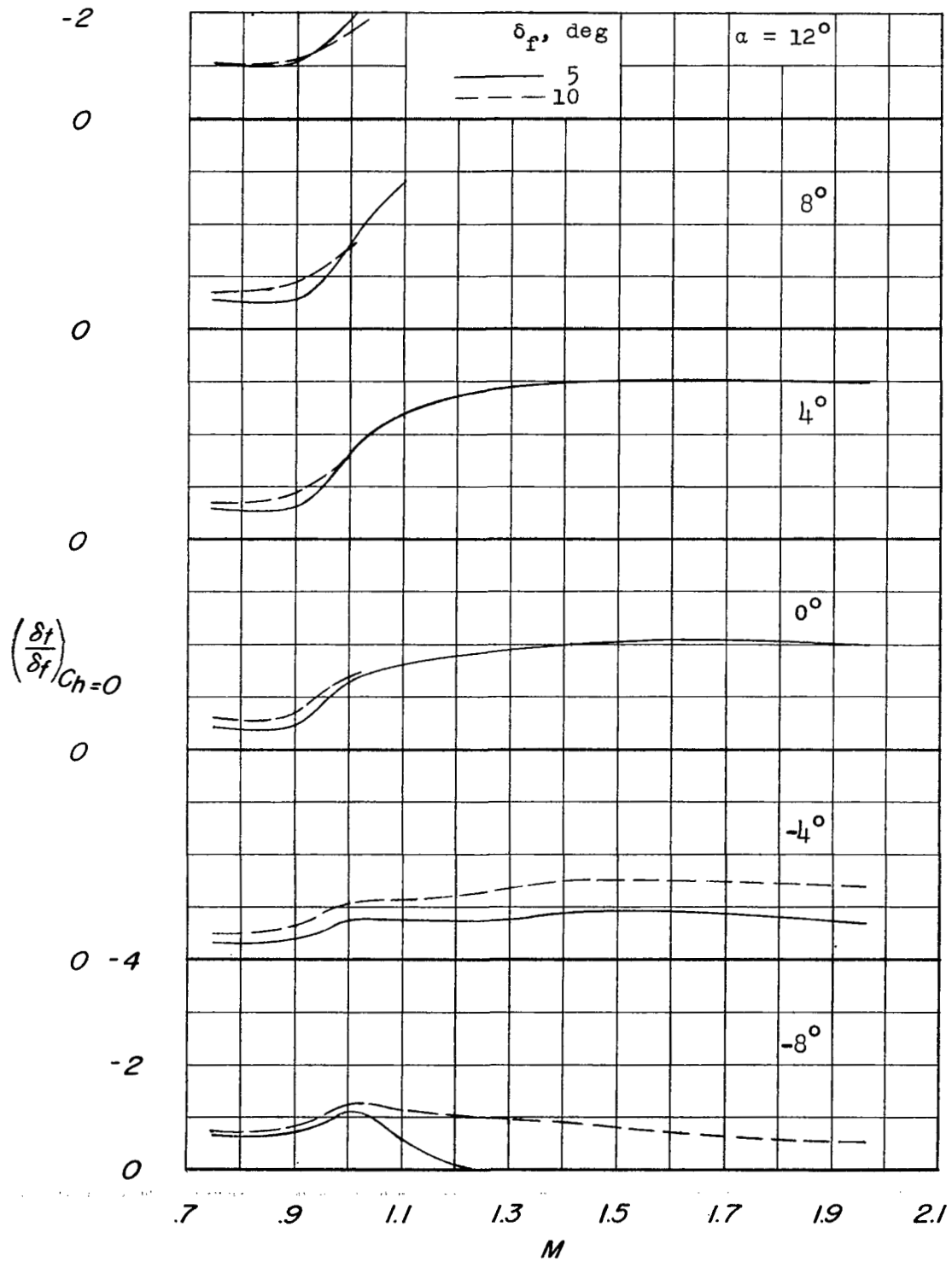

Figure 11.- Variation with Mach number of the ratio of tab deflection to flap deflection required for $C_h = 0$.

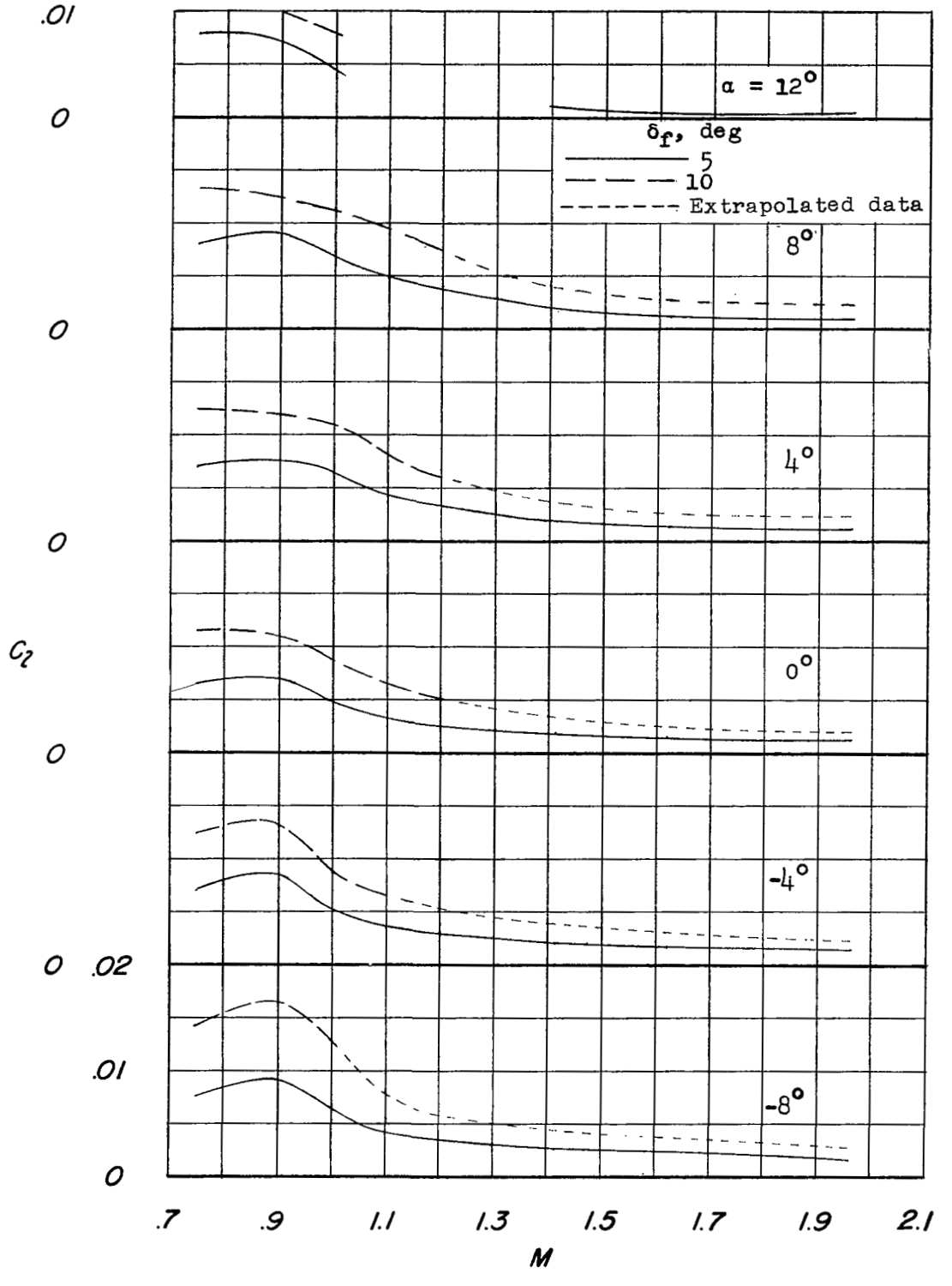

Figure 12.- Variation with Mach number of the rolling-moment coefficient due to flap and tab deflection for $\Delta C_h = 0$.

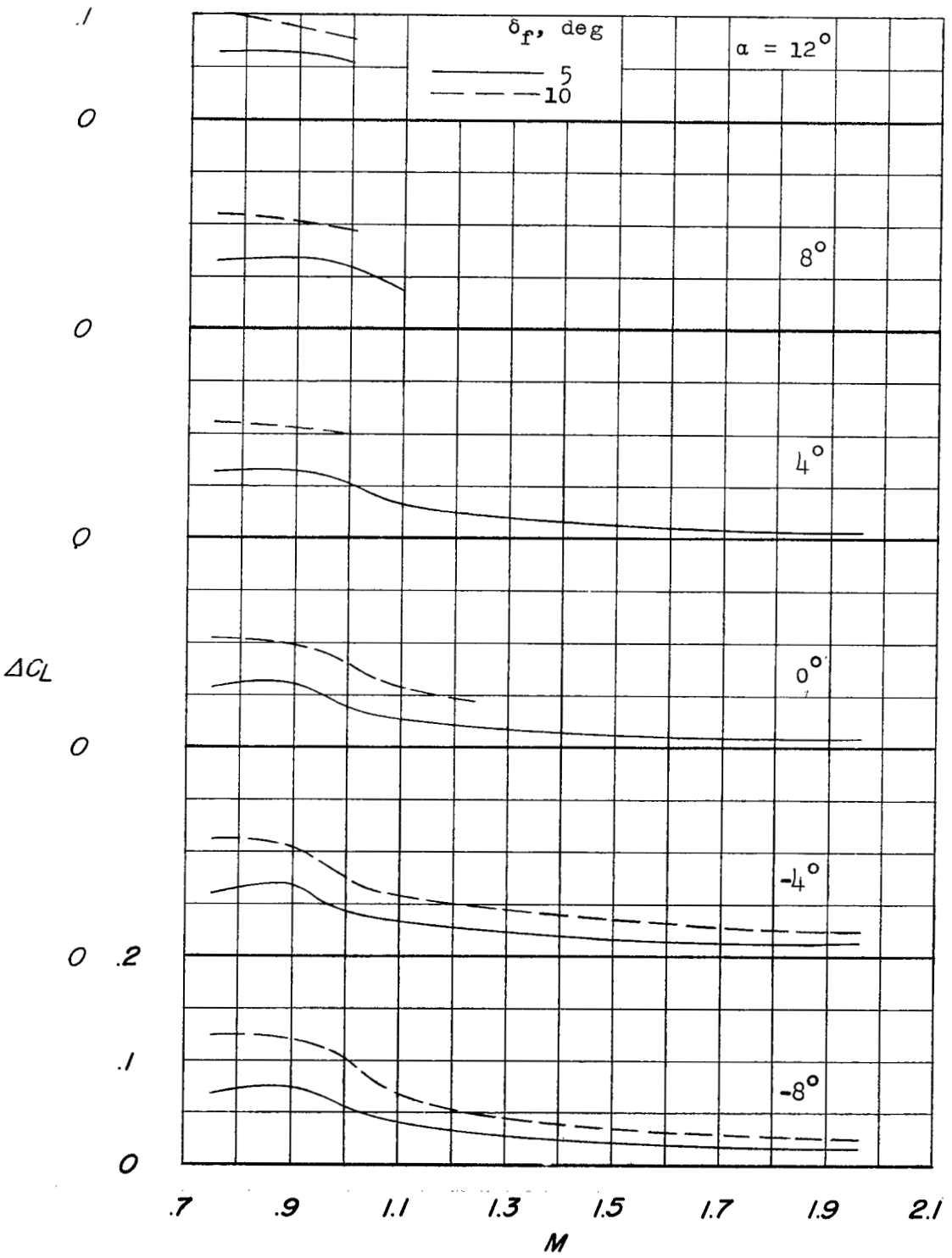

Figure 13.- Variation with Mach number of the increments of lift due to flap and tab deflection for $C_h = 0$.

[redacted]

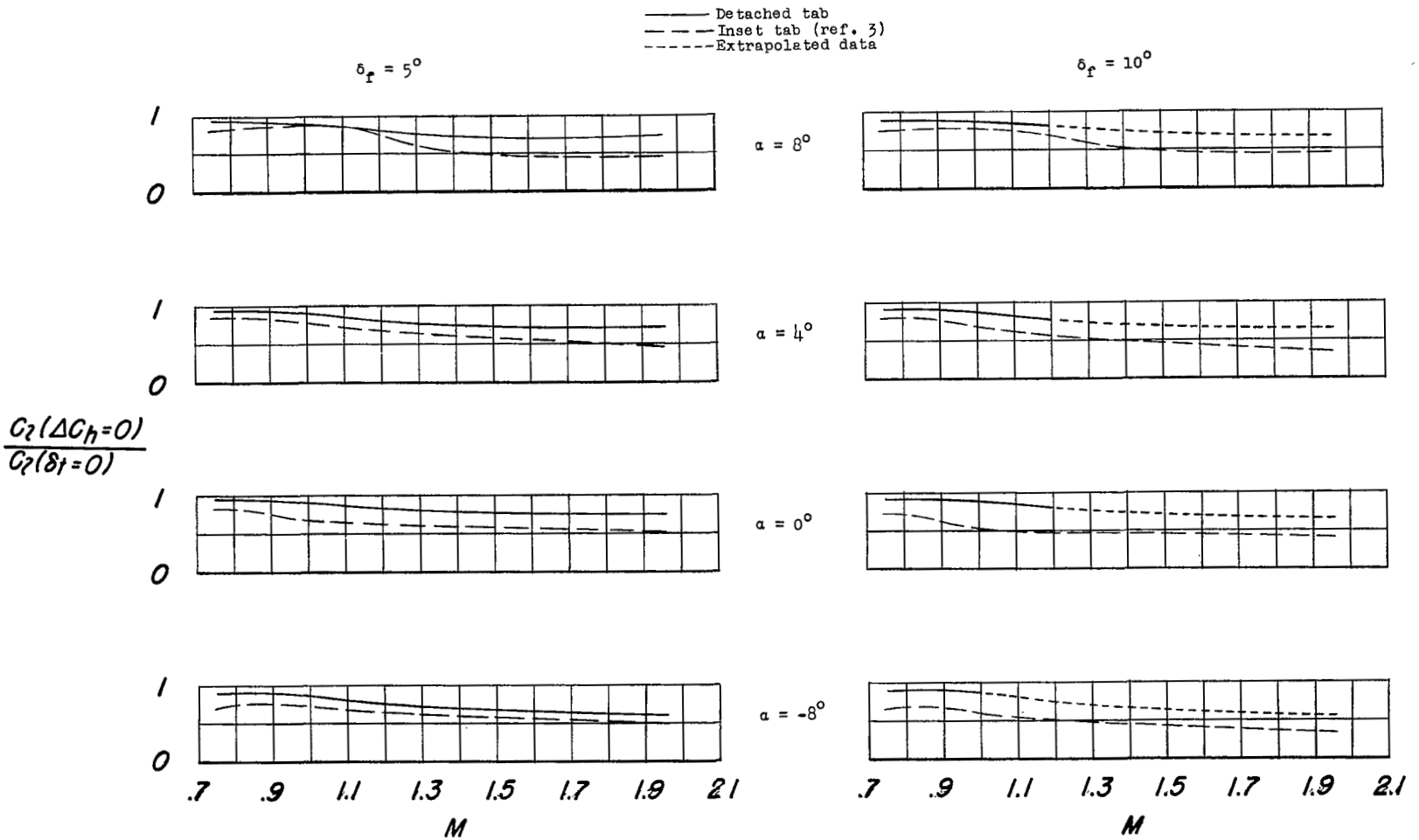

Figure 14.- Ratio of the rolling moment of the flap with the tab deflected for $\Delta C_h = 0$ to that of the flap with the tab undeflected.

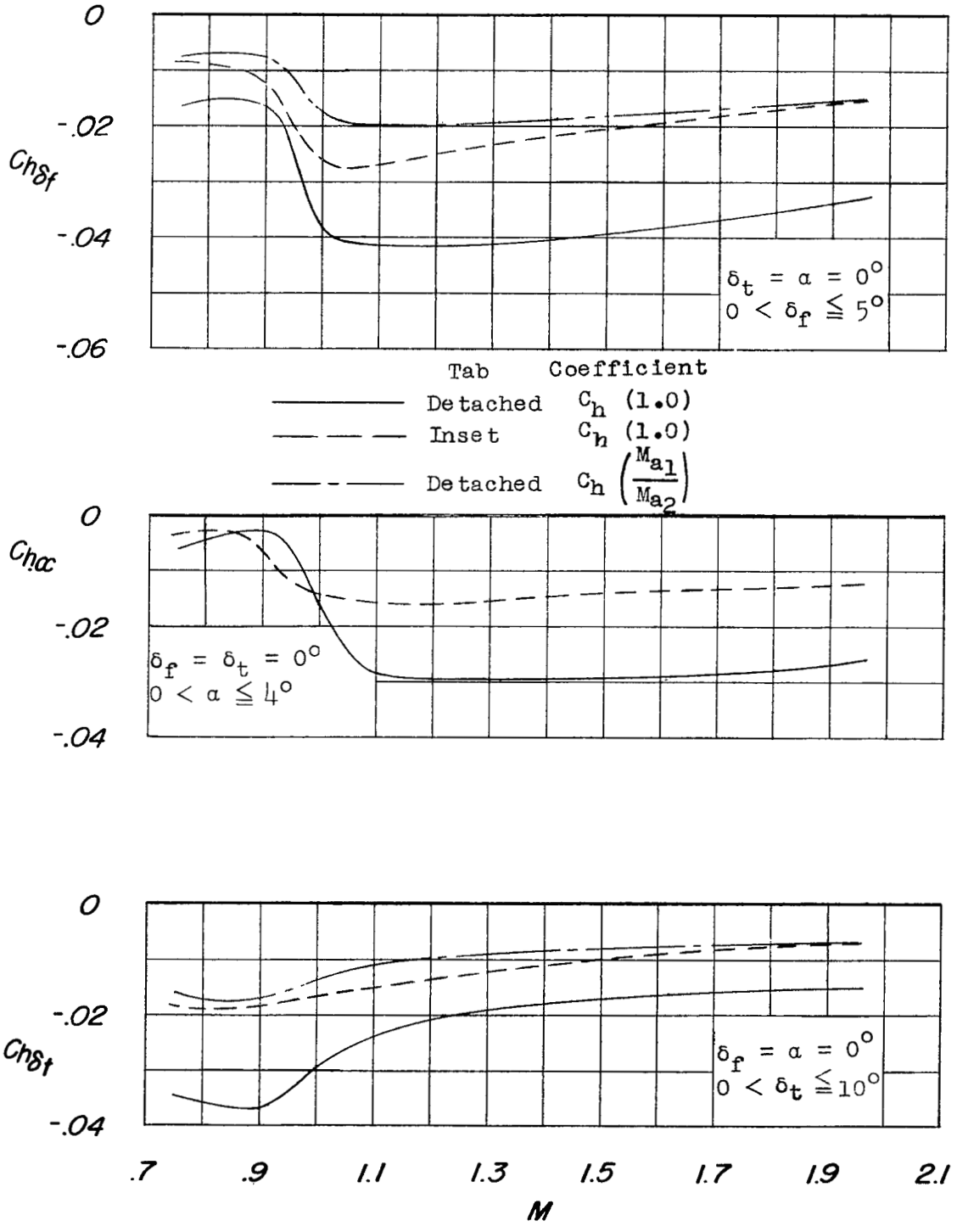

Figure 15.- Variation with Mach number of the slope parameters $C_{h_{\delta_f}}$, C_{h_α}, and $C_{h_{\delta_t}}$.

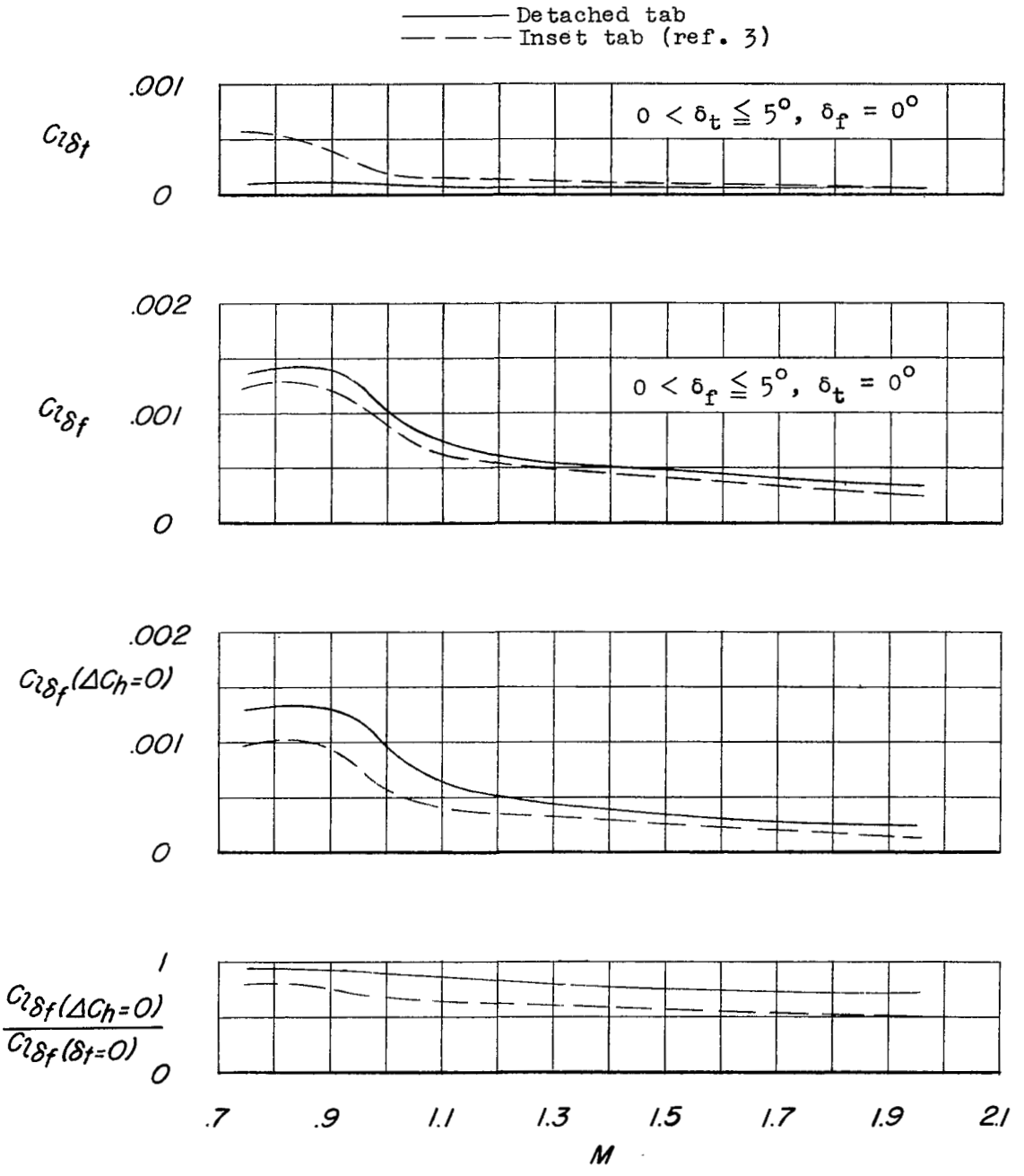

Figure 16.- Variation with Mach number of some flap and tab rolling-moment effectiveness parameters. $\alpha = 0$.

NACA-Langley - 4-1 -55 - 350